



SCHOOL of
GRADUATE STUDIES
EAST TENNESSEE STATE UNIVERSITY

East Tennessee State University
Digital Commons @ East
Tennessee State University

Electronic Theses and Dissertations

Student Works

12-2011

Mesoporous Functionalized Materials for Post-Combustion Carbon Dioxide Capture.

Kolade Omoniyi Ojo
East Tennessee State University

Follow this and additional works at: <https://dc.etsu.edu/etd>

 Part of the [Materials Chemistry Commons](#)

Recommended Citation

Ojo, Kolade Omoniyi, "Mesoporous Functionalized Materials for Post-Combustion Carbon Dioxide Capture." (2011). *Electronic Theses and Dissertations*. Paper 1378. <https://dc.etsu.edu/etd/1378>

This Thesis - Open Access is brought to you for free and open access by the Student Works at Digital Commons @ East Tennessee State University. It has been accepted for inclusion in Electronic Theses and Dissertations by an authorized administrator of Digital Commons @ East Tennessee State University. For more information, please contact digilib@etsu.edu.

Mesoporous Functionalized Materials for Post-Combustion Carbon Dioxide Capture

A thesis

presented to

the faculty of the Department of Chemistry

East Tennessee State University

In partial fulfillment

of the requirements for the degree

Master of Science in Chemistry

by

Kolade Omoniyi Ojo

December 2011

Dr. Aleksey Vasiliev, PhD, Chair

Dr. Yulin Jiang, PhD

Dr. Jeffrey Wardeska, PhD

Keywords: Carbon Dioxide, Hybrid Organic-Inorganic materials, Sol-gel, Mesoporous materials, Amine groups, X-ray diffraction, Small angle X-ray scattering.

ABSTRACT

Mesoporous Functionalized Materials for Post-Combustion Carbon Dioxide Capture

by

Kolade Omoniyi Ojo

Novel highly functionalized hybrid organic-inorganic materials were synthesized by polycondensation of bis[3-(trimethoxysilyl)propyl]amine in presence of cationic and anionic surfactants. Reaction media strongly affected gelation time. Thus, in basic media gelation occurred immediately while acid increased gelation time. Material structures were studied by IR spectroscopy, porosimetry, XRD, and SAXS methods. In spite of the absence of an inorganic linker, obtained bridged silsesquioxanes had mesoporous structure. A material prepared in the presence of dodecylamine as a template had higher surface area and narrow pore size distribution while the use of sodium dodecylbenzene sulfate resulted in formation of mesopores with wide size ranges. Accessibility of surface amine groups in silsesquioxanes was studied for molecules of acidic nature and different sizes: HCl, CO₂ and picric acid. High contents of accessible amine groups in these materials make them prospective adsorbents for post-combustion CO₂ capture.

DEDICATION

This work is dedicated to my parents: my late father, Group Captain Andrew Ajayi Ojo and my mother Mrs. Modupe Ojo. My brothers: Olusegun, Olatunbosun. My sisters: Mrs. Oluwaseyi Adeyemo, Mrs. Oluwatoyin Ososanya, Miss Ifelayo Ojo. My uncle: Honorable Shola Ojo.

ACKNOWLEDGEMENTS

This work was supported by Civil Research and Development Foundation (grant UKC2-2956-KV-08). We thank Dr. Guanci (Eastman Chemical Company) for recording XRD patterns of the materials and Dr. Gomza (Institute of Macromolecular Chemistry, Ukraine) for SAXS study.

I would start by saying a heart-felt thank you to Dr. Aleksey Vasiliev for his mentorship and support during my research, Sir may God richly bless you. I also want to express my sincere appreciation to Dr. Yulin Jiang and Dr. Jeffrey Wardeska for serving as committee members for my thesis. I want to also use this medium to thank the following people: Isaac Agyekum, Antibe Pouliwe, Franklin Ifeanyichukwu Uba, Anne Item, Bahago Nathaniel Atamas, Deborah Hayford, Dr. Daniel Owens, Mary Addy, Guanana Zhou, Thomas Simerly, Paras Pargeni, Lakbub Jude, Ifeoma Ozodiegwu, Dr. Uchenna Egenti, Marian Osei-Mensah Kamasah, Dinci Pennap, Ruth Agbaji, Ayodele Olomosua, Andrew Ashiofu, Nkongho Atem-Tambe, Stanley Jing, Professor A.O Oyewale, Professor (Mrs.) E.B Agbaji, Dr. Rashidat Ayinla, Eme Amba Abu, and Alexander Kamasah for their care and support. Special thanks go to Dr. Cassandra Eagle, Dr. Ray Mosheni, Tom Webster, Dr. Cook, Dr. Chu-Ngi Ho, and Jillian Quirante for their love and care.

CONTENTS

	Page
ABSTRACT.....	2
DEDICATION.....	3
ACKNOWLEDGEMENTS.....	4
LIST OF TABLES.....	8
LIST OF FIGURES.....	9
Chapter	
1. INTRODUCTION.....	10
Global Warming.....	10
CO ₂ Capture, Storage, and Sequestration.....	12
Using Liquid Amine Based Compounds for Chemical Absorption.....	13
Description of a Typical Amine Based Absorption Process.....	17
Examples of Amines and Silanes Used in the Synthesis of Solid Supported Amine Adsorbents.....	18
Organic-Inorganic Functionalized Materials as Prospective Adsorbents for CO ₂ Capture.....	19
Bridged Silsesquioxanes.....	26
General Background of Sol-Gel Chemistry.....	28

Research Objective	29
2. EXPERIMENTAL	30
Reagents	30
Precursor	30
Surfactants.....	30
Other Chemicals	30
Preparation of Sample 1	32
Preparation of Sample2	32
Characterization	33
Potentiometric Titration.....	34
CO ₂ Adsorption and Desorption on Samples.....	36
Percentage of Water Adsorbed Per Dry Samples.....	36
3. RESULTS AND DISCUSSION	37
Synthesis of Samples	37
Total Contents of Amino Groups	37
FT-IR Spectroscopy	38
Porous Characteristics of Samples	38
X-ray Powder Diffraction Patterns of Samples	39
Small Angle X-ray Scattering	40
Transmission Electron Microscopy of Samples	40
Relative Basicity of Samples	41

Carbon Dioxide Adsorption	41
Adsorption Capacity on Water	42
Conclusion	44
REFERENCES	44
APPENDICES	52
Appendix A: BET Adsorption Isotherms of Samples 1&2	52
Appendix B: TEM Image of Sample 1	53
Appendix C: TEM Image of Sample 2	54
Appendix D: X-Ray Powder Diffractogram of Sample 1	55
Appendix E: X-Ray Powder Diffractogram of Sample 2	56
Appendix F: FT-IR Spectra of Samples 1 & 2	57
Appendix G: Confirmation of the Molecule of BTMSA in the Conformation with Minimized Energy	58
Appendix H: SAXS Curves of Samples 1&2 a-1 and b-2	59
VITA	60

LIST OF TABLES

Table	Page
1. Structures of amines and silanes used in the synthesis of solid supported amine adsorbents.....	18
2. Porous characteristics of bridged silsesquioxanes	39
3. Characteristics of silsesquioxanes	42
4. Results of the % >NH groups accessible.....	43

LIST OF FIGURES

Figure	Page
1. Carbamate formation by the reaction of CO ₂ with primary and secondary amines	15
2. Mechanism of the reaction between CO ₂ and tertiary amines	16
3. Schematic of a typical amine based absorption process	17
4. Typical example of a Sol-Gel synthesis	29
5. Structure of BTMSPA	30
6. Structure of DDA	30
7. Structure of DDS	31
8. Structure of Picric Acid	31
9. Structure of KHP	31

CHAPTER 1

INTRODUCTION

Global Warming

Global warming is defined as the increase in the Earth's average surface temperature as a result of the build-up of greenhouse gases in the atmosphere. The atmosphere has a natural supply of greenhouse gases and these gases help in keeping the surface of the Earth warm enough for humans to live on by capturing heat. In the same way the greenhouse effect plays a vital role in ensuring that the planet would be a habitable place for humans and that it doesn't turn out to be a wasted frozen land. However, human activities such as burning of fossil fuels (e.g. coal, oil, and natural gas), which have a high carbon content, generate carbon dioxide and its concentration in the atmosphere tends to increase. Carbon dioxide is known to be the leading cause of global warming. Global warming is known to negatively impact the world around us. Examples of the catastrophic effects global warming has on the world includes extreme heat waves, extreme allergies, negative impact on winter weather, extreme drought, wildfires, floods, hurricanes, coral bleaching, shifting habitat, shrinking of the arctic sea, melting of glaciers, spread of diseases, worsening air quality, and a great decline in the polar bear population . In general, global warming has impacted negatively on the living conditions of both humans and animals and something has to be done to overcome this greenhouse effect [1].

Kessel in his studies showed that the world's primary energy usage amounts to 8.38 billion tons oil equivalent (OE) (1996) and it is projected to rise by 1.3 percent annually for highly industrialized nations of the world and by up to 9.2 percent annually for developing nations. According to his research, it is estimated that the continuous usage of fossil [2] energy

will lead to a further increase in the mean global temperature within the next 50 to 100 years. This will in turn tend to increase CO₂ emission, which is known to contribute to global warming [2]. The total amount of carbon on the Earth has remained the same and its allocation among the lithosphere, atmosphere, and biosphere was moderately equal until the time of the industrialized civilization. The level of carbon dioxide in the atmosphere is still rising. Carbon dioxide levels have gone up from 280 ppmv in the 1000s to 295 ppmv in 1900s as revealed in the Antarctica ice core data. “Carbon dioxide levels further elevated to 315 ppmv in 1958 and elevated again to 377 ppmv in 2004 as reported by the core data logged in Hawaii” [3]. Several ways have been employed in lowering the levels of CO₂ emissions in the atmosphere. These include avoiding activities that give off excess CO₂, enhancing energy capabilities (for example combined cycle generation, isolation of buildings, vehicles), replacing activities that lead to higher evolution of CO₂ by less CO₂ evolving ones and substituting CO₂-emitting processes by CO₂- free ones [2]. Adsorption is one of the promising ways used for isolating carbon dioxide from a mixture of gases, and many studies have been carried out on the sequestering of carbon dioxide by adsorption in the last 20 years. Different types of materials that can be employed as prospective adsorbents have been examined. Examples of these adsorbent materials include activated carbons [4,5], silica adsorbents [6,7], carbon nanotubes [8], nanoporous silica-based molecular baskets, [9] and zeolites [10,11].

The intergovernmental panel on climate change (IPCC) special report on carbon dioxide capture and storage concludes that adsorption processes have been used for the separation of CO₂ from synthesis gas for the manufacture of hydrogen gas. According to this report, which was based on a mathematical model and data from pilot-scale experimental installations, it was revealed that a full-scale industrial adsorption process will be possible and the development of

novel materials that would efficiently adsorb CO₂ would undeniably improve the competitiveness of adsorption processes in flue gas applications [12].

CO₂ Capture, Storage, and Sequestration

Separation of CO₂ from flue gas requires a lot of energy. Several methods have been used for the separation and capture of CO₂ and these methods are divided into three categories: post-combustion process which is used in common coal-fired power plants, pre-combustion process which has been used in gasification and oxy-fuel combustion process. The oxy-fuel combustion is also known as oxy-firing or oxy-combustion. The advancement in CO₂ separation and capture resulted in the evolution of other methods used in the capture of this anthropogenic gas.

Techniques such as chemical-looping combustion traditionally known as CLC have been employed to reduce the intricacy of separating CO₂ from a gas stream to a great extent. A study by Holloway recommends that CO₂ capture and geological accumulation is an evolving method that could be used to lessen carbon dioxide emissions into the atmosphere from very large activity installations such as fossil fuel-fired power stations by 80-90 percent because this process encompasses the capture of carbon dioxide at a large industrial establishment, its mobility to a geological accumulation site and its continuous isolation in a geological accumulating reservoir [13]. This technique is believed to help in lowering emissions from fossil fuels that are likely to remain the bulk source of primary energy in the future.

Distribution of carbon dioxide in deep oceans, depleted oil and gas fields, deep saline formation, and recovery of enhanced oil, gas, and coal bed methane are present techniques used in its isolation. The pumping of carbon dioxide in deep geological structures is a traditional drill of many oil refining industries because the liquid petroleum and methane retrieval processes

from the storage sites involves re-injecting carbon dioxide from exhaust gases in order to shove oil from storage sites to the exterior for further separation. The transmutation of greenhouse gases into fertilizers like NH_4HCO_3 is an upcoming and innovative technology used for introducing carbon dioxide into the soil and subsoil Earth layers [13].

Using Liquid Amine Based Compounds for Chemical Absorption

Monoethanolamine (MEA) absorption procedure for the isolation of carbon dioxide has been studied to a great extent. Numerous natural gas establishments use monoethanolamine for the absorption of carbon dioxide from natural gas streams. The various marketable monoethanolamine absorption approaches employed in the removal of carbon dioxide from combustion flue gas stream, permits the interaction of the MEA solution with the flue gas in an absorber where carbon dioxide is being absorbed by the solution containing the MEA and flue gas. This technique encompasses the reaction of carbon dioxide with monoethanolamine in the gas stream to form monoethanolamine carbamate, and this carbamate solution is then conveyed to a stripper where it is burned up a second time to set free carbon dioxide which is almost pure. However, this process is not economically viable as it necessitates the use of large apparatus and also necessitates the use of elevated energy. A schematic for a representative amine based absorption method is shown in Figure 3.

Diethanolamine (DEA) and methyl diethanolamine (MDEA) are mostly used as absorbents for carbon dioxide capture. A reaction mechanism was proposed by Grey et al.[3] in 2005. According to their proposed mechanism, it was shown that the bulk of the carbon dioxide captured will lead to the production of bicarbonate in the liquid amine capture network. In aqueous medium, a 2 mol-amine/mol carbon dioxide is necessary for the production of stable

bicarbonate compounds leading to the capture of carbon dioxide. Hybrid amines have been used in order to generate a solution composed of tertiary and primary amines or tertiary plus secondary amine that reserve significantly most of the reactivity of primary amines or secondary amines at comparable or lessened flow rate but affords a lessened rejuvenation cost comparable to those of tertiary amines [3].

The reaction of carbon dioxide with amines is ruled by distinct mechanisms. Primary and secondary amines can react directly with carbon dioxide to generate carbamates via the generation of zwitterionic intermediates [14]. The zwitterionic mechanism for the generation of carbamates from the reaction between carbon dioxide and a primary amine was described by Caplow [15]. The initial step of the reaction involves the lone pair of electrons on the amine attacking the carbonyl carbon of carbon dioxide to generate a zwitterion. A free base then removes a proton from the zwitterion to produce a carbamate as shown in Figure 1. However, in an aqueous amine surrounding, a second amine can be the base or water or OH^- . This mechanism is useful to secondary and primary amines [16]. Under anhydrous conditions, the greatest amine efficacy of an amine adsorbent is 0.5 mol CO_2 per mol N. Amine efficacy can be defined as the number of moles of CO_2 adsorbed per mass unit divided by moles of nitrogen per mass unit. This amine efficacy often gives a reflection of an adsorbent's efficacy in relation with its capability. However, under wet conditions, where water can behave as a base, the greatest amine efficiency is 1.0 mol CO_2 per mol nitrogen [14].

Tertiary amines react with carbon dioxide via a different mechanism. This mechanism involving the base-catalyzed hydration of CO_2 for the reaction of tertiary amines with CO_2 was first described by Donaldson [17] and was subsequently modified by Kenig [18]. In this mechanism, tertiary amines catalyze the production of bicarbonates because they do not react at

once with CO₂. The first step of the reaction encompasses the dissociation of water by tertiary amines to generate quaternary cationic species and OH⁻. The OH⁻ then reacts with CO₂ to produce a bicarbonate anion. The final step of the mechanism reveals the ionic association of the protonated amine and bicarbonate as shown in Figure 2. Primary and secondary amines are capable of reacting with water and CO₂ in this way.

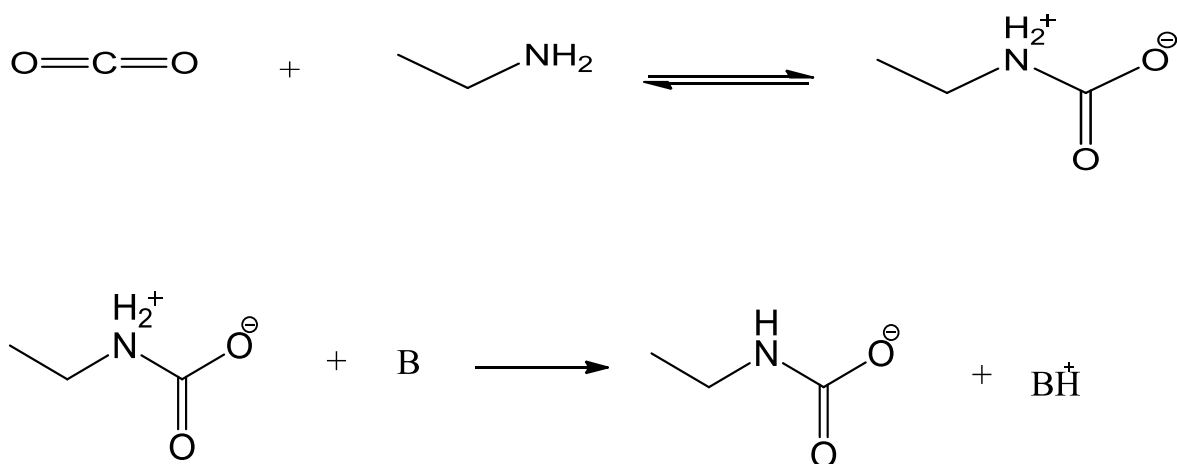


Figure 1. Carbamate formation by the reaction of CO₂ with primary and secondary amines

[14]

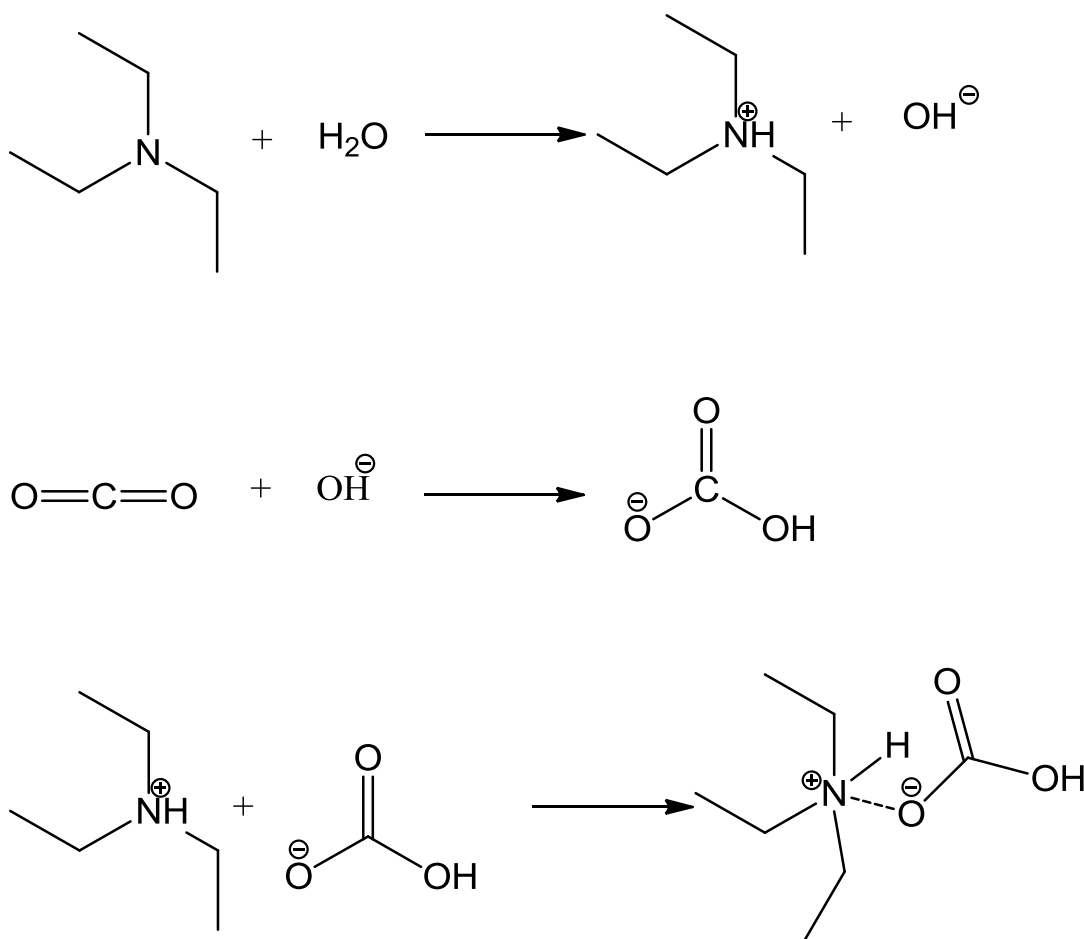


Figure 2. Mechanism of the reaction between CO₂ and tertiary amines [14]

There are numerous setbacks involved when liquid amines are used as adsorbents for carbon dioxide capture from flue gas. These setbacks include: (1) there's always a lessened carbon dioxide loading capacity; (2) there's always a heightened corrosion rate of apparatus used; (3) amines are typically destroyed by SO₂, NO₂, HCl, HF, and oxygen in flue gas which induces an elevated absorbent makeup rate; (4) there is always elevated energy consumption amidst elevated temperature absorbent rejuvenation [3]. The need for the development of solid based mesoporous adsorbents with surface functional groups for the capture and sequestration of carbon dioxide has drawn a lot of attention.

Description of a Typical Amine-Based Absorption Process

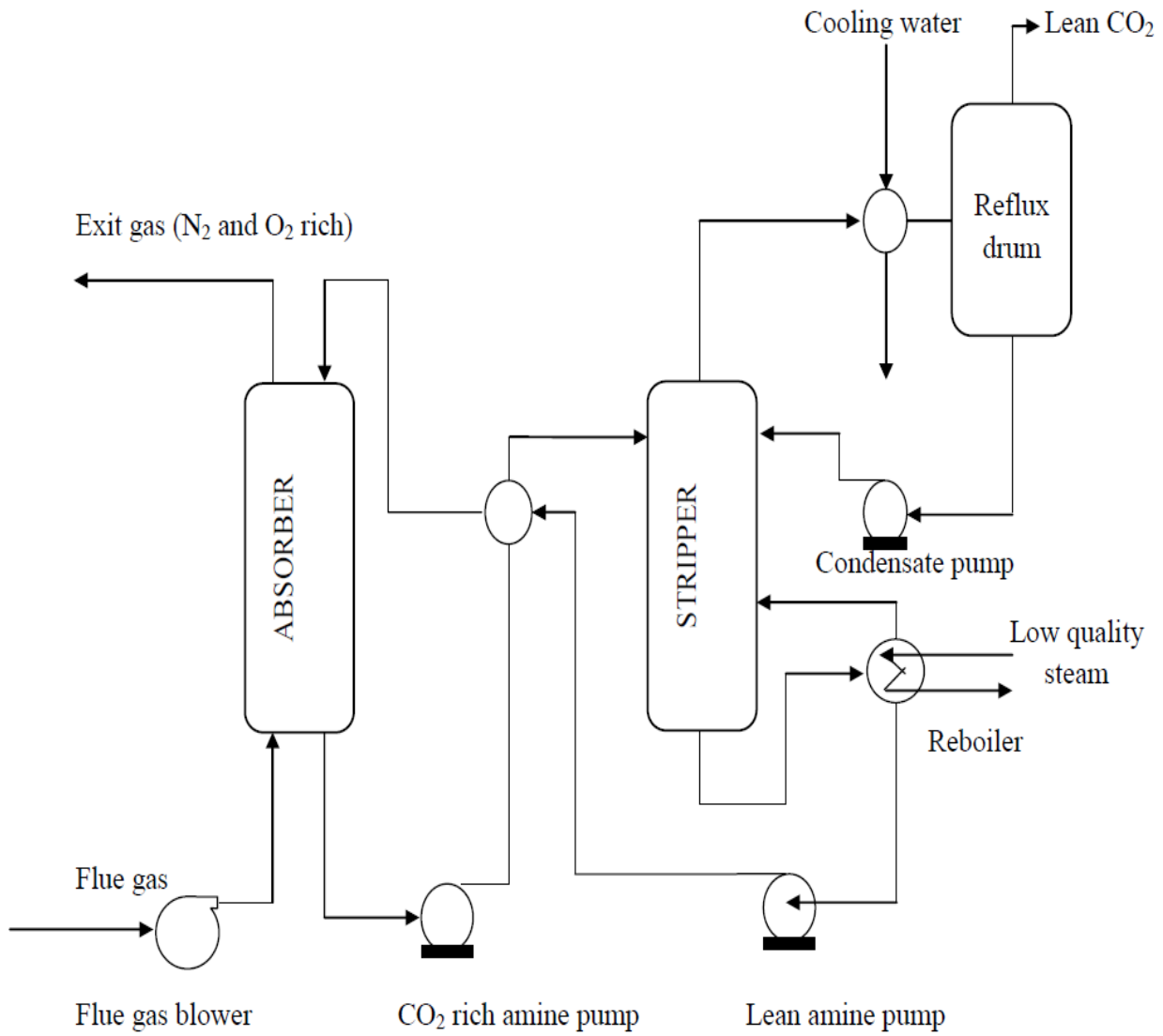


Figure 3. Schematic of a typical amine based absorption process

Examples of amines and silanes used in the synthesis of solid supported amine adsorbents

Table 1. Structures of Amines and silanes used in the synthesis of solid supported amine adsorbents [14]

Amine type	Support	Product
	Silica	
	Silica	
	Silica	
	Silica	
	Activated Carbon	
	Activated Carbon	

Organic-Inorganic Functionalized Materials as Prospective Adsorbents for CO₂ Capture

According to the Institute of Materials Chemistry at Vienna University of Technology, “organic-inorganic materials are materials created by blending organic and inorganic building blocks. The evolution of these material prototypes, which have already established diverse applications, is one of the utmost accomplishments of sol-gel science. The catch is to prepare materials with novel merging of properties by mixing organic and inorganic building blocks on a molecular level. Organic-inorganic hybrid materials which have been synthesized by the sol-gel method have swiftly become an interesting novel area of research in materials science” [19].

Hybrid organic-inorganic mesoporous materials containing surface functional groups have found many applications in chemistry, in particular as catalysts [20,21] and adsorbents [22]. The performance of these material types depends on contents of the functional groups accessible for molecules of reactants or adsorbates. Most synthetic methods of preparation of these materials fall into two categories; sol-gel procedure and post-synthetic grafting of organic compounds [23]. However, both techniques do not provide high contents of organic groups on the surface. Loading of organic molecules on the surface of porous materials by grafting is restricted by steric hindrances [24]. Sol-gel method allows incorporation of any amount of organic trialkoxysilane precursors during their mixed polycondensations with an inorganic linker, usually tetraethoxysilane (TEOS). However, porosity of the products strongly depends on the contents of the organic precursor. Pendant organic groups reduce resistibility of pore walls against interporous capillary forces during the drying process thus resulting in shrinkage and loss of porosity [25]. In particular, polycondensation of (3-aminopropyl)trimethoxysilane without a linker gives a product with $S_{\text{BET}} < 6 \text{ m}^2/\text{g}$ [26,27]. To present time no mesoporous materials were obtained from precursors with pendant organic groups without the use of an inorganic linker

[28]. Addition of TEOS is necessary to preserve mesoporous structure of the products from collapse. A drawback of this method is low contents of functional groups in the obtained material due to reduced ratio between organic and inorganic phases. Thus, a typical loading of amine groups in mesoporous silsesquioxanes usually does not exceed 2.7-3.4 mmol/g [29]. Attempts to increase their amine contents by reducing the concentration of TEOS results in loss of porosity.

Various amine types have been researched for impregnation into silica supports. These amines typically range from simple monoamines to aminopolymers, but poly(ethyleneimine) is commonly used. Poly(ethyleneimine) can either be a branched aminopolymer containing a mixture of primary, secondary, and tertiary amines or a linear amino polymer of secondary amines with primary amine termini [14]. Structures of amines and silanes used in the synthesis of solid supported amine adsorbents are shown in Table 1. It was shown by Gray et al.[6] in 2005 that the trapping of carbon dioxide from simulated flue gas can be carried out by using immobilized and aminated–Santa Barbara Amorphous Silica-15 (SBA-15) solid adsorbents. SBA-15 is a mesoporous silica material which has a uniform pore size of 21 nm and a surface area of 200~230 m²/g. Their results suggested that immobilized secondary amines have a higher potential for the capture of carbon dioxide from simulated flue gas streams in comparison to primary amines. Therefore, higher amine content and the use of secondary ethyleneamine type adsorbents enhances carbon dioxide capture capacity among a wide variety of immobilized amine adsorbents that have been explored so far [6].

Huang et al.[30] in their effort to develop selective solid adsorbents for acidic gas isolation from natural gas composites in 2003 synthesized amine-surface-modified silica xerogel and MCM-48 materials. These materials consist of large number of basic amine functional groups on their surfaces. The huge amount of basic amine functional groups present makes these

materials selective when bonding with acidic substrates like carbon dioxide and hydrogen sulfide gas. Further work done has revealed that the adsorption-desorption isotherms of the gases and the thermogravimetric analysis results of the adsorbents showed that these sorbents can be rejuvenated completely under mild conditions just as those employed in temperature swing adsorption processes. The effect of moisture on the adsorption of the acidic substrates was also investigated by Huang and co-workers, where they used temperature programmed desorption mass spectroscopy and infrared spectroscopy techniques and the results he obtained indicated that the presence of water vapor increased the amount of carbon dioxide absorbed by a factor of 2. The success of the adsorbents depends on successful grafting of amine functional groups onto the surface via the interaction of the surface hydroxyl groups of the reactant materials with (3-aminopropyl)silanes. Huge amounts of amine functional groups attached to the surface of these adsorbents, high surface area and hydroxyl ion contents are predominantly responsible for their potential to adsorb carbon dioxide and hydrogen sulfide [30].

Khatri et al. [31] in 2005 studied carbon dioxide capture by diamine-grafted SBA-15. They studied the adsorption and desorption of carbon dioxide on this amine grafted SBA-15 by infrared spectroscopy coupled with mass spectrometry. Diamine was grafted onto a Santa Barbara Amorphous Silica-15 (SBA-15) surface by the reaction of [N-(2-aminoethyl)-3-aminopropyl]trimethoxysilane with the surface OH. Carbon dioxide is adsorbed on the diamine-grafted SBA-15 as a bidentate carbonate and bidentate and monodentate bicarbonates at 25 °C. Temperature-programmed desorption revealed that when monodentate and bidentate bicarbonates are bound to a diamine-grafted SBA-15 surface, they are strongly held to this surface compared to only when a bidentate bicarbonate is bound to this surface. It was further revealed that the amount of carbon dioxide desorbed from the carbonate and bicarbonate

between 30 and 120 °C was 2 times more than that of carbon dioxide adsorbed/desorbed during each cycle of the concentration-swing adsorption desorption. Their conclusion was that carbon dioxide adsorbs on the primary and secondary amine functional groups generating carbonates, bicarbonates, and carbamic acid species.

Xu et al. [32] in 2002 developed a nanoporous solid adsorbent that served as a molecular basket for carbon dioxide capture in the condensed form. In their work, polyethylenimine (PEI)-modified mesoporous molecular sieve of MCM-41 type (MCM-41-PEI) was prepared and tested as an adsorbent for carbon dioxide capture. The physical properties of the adsorbents were characterized by X-ray powder diffraction (XRD), N₂ adsorption /desorption, and thermogravimetric analysis (TGA). Their characterizations showed that the MCM-41 preserved its structure after loading with the PEI, and the PEI was uniformly dispersed into the channels of the molecular sieve. The carbon dioxide adsorption capacity was reported as 215 mg-CO₂/g-PEI with MCM-41-PEI-50 at 75 °C, which was 24 times higher than that of MCM-41 and it is twice that of the pure PEI. Loading different substances with affinities for different gases to a mesoporous molecular sieve is a novel idea and can be used to develop different types of high selective, high- adsorption-capacity molecular baskets [32]. Knowles et al. were able to functionalize mesoporous silica substrates with (3-aminopropyl)trimethoxysilane and [N-(2-aminoethyl)-3-aminopropyl]trimethoxysilane to produce hybrid materials suitable for the capture of carbon dioxide. They combined TGA/DTA to determine carbon dioxide adsorption capacities and heats of adsorption. At 20 °C, they observed a reasonable carbon dioxide adsorption capacity under both dry and wet conditions while the heats of adsorption differed greatly. The reason for the differed heats of adsorption relates to the simultaneous formation of bicarbonate species under the wet condition [33]. Knowles et al. again prepared a series of amine functionalized

silica by modification of different mesoporous silica substrates with (3-aminopropyl)trimethoxysilane and [N-(2-aminoethyl)-3-aminopropyl]trimethoxysilane. The extent of surface functionalization was found to depend on the size of the reagents, diffusion of reagents to the surface, silanol concentration on the substrate surface, and on both the available surface area and porosity of the substrate. Their synthetic procedure led to the formation of products with very high nitrogen content on the basis of mass relative to the analogous amine-functionalized silica materials reported to date. The higher adsorption capacities and higher heats of adsorption suggest that adsorption on the amine-functionalized materials occurred via the ammonium carbamate formation only with high aminopropyl loading. It was found that at lower loadings of aminopropyl, adsorption of carbon dioxide occurs by classical physisorption. Their results also shows that the use of longer [N-(2-aminoethyl)-3-aminopropyl]trimethoxysilane tethers provides superior carbon dioxide adsorption capacities at 293 K on a unit mass or unit surface area basis. The drawback is that the method lowers the amine efficiency. These materials are able to adsorb carbon dioxide in the presence of moderate amounts of water. However, the lower adsorption capacity observed for the [N-(2-aminoethyl)-3-aminopropyl]trimethoxysilane maybe as a result of poorer access to the amine sorption sites [33]. Knowles et al. again synthesized a series of 3[2-(2-aminoethylamino)ethylaminopropyltrimethoxysilyl(DT) functionalized silica by modification of different mesoporous silica substrates with 3[2-(2-aminoethylamino)ethylaminopropyltrimethoxysilane(TRI) and these materials were characterized to determine their extent of surface functionalization and to assess their potentials as adsorbents for carbon dioxide capture. Their studies again show that the extent of surface functionalization depends on the diffusion of reagents to the surface, the concentration of the

silanol on the surface of the substrate, and both the available surface area and porosity of the substrate. The synthetic methodology used generally leads to hybrid materials with fewer tethers per unit substrate surface area but more N per unit mass and more N per unit product surface area than the analogous (3-aminopropyl)silyl and [N-(2-aminoethyl)-3aminopropyl]trimethoxysilyl functionalized hybrid materials. However, under moist conditions, the amount of carbon dioxide adsorbed onto 3[2-(2-aminoethylamino)propyltrimethoxysilyl (DT) functionalized silica material is reduced and this reduction in the carbon dioxide capacity may be due to the poor availability of weak physisorption sites as a result of the preadsorption of water [34].

Peter and co-workers in their work coated a pore-expanded MCM-41 (PE-MCM-41) mesoporous silica material with 3[2-(2-aminoethylamino)ethylamino]propyl trimethoxysilane (TRI) and studied the carbon dioxide adsorption capacity from nitrogen gas as a function of the amount of TRI and water per gram of support added to the grafting mixture. The TRI grafted PE-MCM-41 adsorbent exhibits a 2.65 mmol/g adsorption capacity at 25 °C and 1.0 atm for a dry 5 % carbon dioxide in a nitrogen feed mixture [35].

Zhao et al. synthesized a range of propyl amine modified mesoporous silica materials and a specific loading of over 4 propylamine per nm² was achieved by careful optimization. They attached propyl-bis(2-hydroxyethyl)amine and propyl-N,N-dimethylacetamidine species to mesoporous silica materials for the first time. A carbon dioxide adsorption capacity of 1.4 mmol/g at 25 °C and 1 atm was achieved for the silica materials modified with the propyl amine functional groups [36].

Pirngruber et al. has shown that silica materials grafted with mono-, di- or triamines have isotherms with moderate curvature but with low absolute sorption capacity. However,

polyamines impregnated on silica materials lead to a high carbon dioxide adsorption capacity but with a problem of regeneration. Primary amines are the strongest adsorption sites for carbon dioxide capture in flue gases [37]. Bhagiyalakshmi et al. have successfully synthesized novel octa(aminophenyl)silsesquioxane grafted SBA-15 mesoporous silica, and they observed a carbon dioxide adsorption capacity of 80 mg/g of adsorbent over the Cl-SBA-15/50 % octa(aminophenyl)silsesquioxane. They also observed that the adsorbent was recyclable, selective, and thermally stable [38].

Gray et al. used an immobilized tertiary amine solid sorbent to study the carbon dioxide capture capacity from a simulated flue gas stream. The tertiary amine immobilized in this solid substrate was 1,8-diazabicyclo-[5.4.0]-undec-7-ene (DBU). The carbon dioxide adsorption capacity of this immobilized DBU solid sorbent prepared was 3.0 molCO₂/kg of adsorbent at 298 K. They further showed that the carbon dioxide adsorption capacity was reduced to 2.3 molCO₂/kg of adsorbent at a critical working temperature of 338 K [39].

Zelenak et al. modified SBA-12 mesoporous silica with 3-aminopropyl (AP), 3-(methylamino)propyl (MAP) and 3-(phenylamino)propyl (PAP) ligands and they found out that the electronic effects in these different ligands resulted in different surface basicity of the modified SBA-12 mesoporous silica material. They observed carbon dioxide sorption capacities of 1.04 mmol/g for sample SBA-12/AP, 0.98 mmol/g for sample SBA-12/MAP and 0.68 mmol/g for sample SBA-12/PAP. It was concluded that grafting of the surface of SBA-12 mesoporous silica with amine functionalities resulted in different base strengths of the surface which played an important role in the chemical fixation of carbon dioxide. Their results showed that a higher basicity of amino ligands increases the efficiency of sorbents with respect to carbon dioxide [40].

Kim and co-workers [41] studied the CO₂ adsorption properties of several amines attached to MCM-48 silica material. In their work, they attached aminopropyl, pyrrolidinepropyl, polymerized aminopropyl groups, and polyethyleneimine to the pore surface of the MCM-48 silica material and studied their various CO₂ adsorption properties. They concluded that CO₂ adsorption capacity was highest when aminopropyl groups were attached to the MCM-48 silica material due to the greater accessibility of the amine groups by CO₂.

Hiyoshi et al. [42] synthesized novel adsorbents for CO₂ capture by grafting different aminosilanes on mesoporous silica SBA-15. They were able to compare the CO₂ adsorption capacities of these aminosilane modified SBA-15 types in the presence and absence of water vapor. Their results showed that there was a linear correlation between adsorption capacities and surface densities of amines. The higher the surface densities of amine groups, the higher would be the amine efficiency on such adsorbents. Hiyoshi and co-workers [43] again used IR spectroscopy to elucidate the adsorption state of CO₂ on aminosilane modified SBA-15. IR studies revealed that CO₂ was adsorbed on the aminosilane modified material by forming an alkylammonium carbamate in which two atoms of nitrogen of an amine plays a vital role in the adsorption process. They concluded that the CO₂ adsorption capacity also increases with increasing number of amine groups on the surface of the adsorbent.

Bridged Silsesquioxanes

Classes of hybrid organic-inorganic materials called bridged polysilsesquioxanes are employed for so many things, ranking from surface modifiers and coatings to catalysts and membrane materials. Hybrid materials fall in the boundary of organic and inorganic spheres. These material types provide choice opportunities not only in the blending of the essential

attributes from both domains but to design completely novel mixtures with matchless attributes [44]. Bridged polysilsesquioxanes is a family of hybrid organic-inorganic materials prepared by sol-gel processing of monomers to provide a changeable organic bridging functional group and many trifunctional silyl groups [45-49]. The stability of a porous structure can be increased by the use of bridged bis-trialkoxysilanes [50-52]. In this case, shorter bridges provide higher rigidity of the network and thus, higher porosity of the materials [23]. In contrast, longer flexible bridges do not favor porosity and such materials usually have reduced surface area.

Polysilsesquioxanes can be made as gels, films, or fibers. The organic functional group which is covalently bonded to the trifunctional silicon groups through a Si-C bond can be varied in length, rigidity, geometry of substitution, and functionality. Because the organic functional group remains an essential part of the material, variation in its length, rigidity, geometry of substitution and functionality provides an opportunity to regulate bulk attributes such as porosity, thermal stability, refractive index, optical clarity, chemical resistance, hydrophobicity, and dielectric constant [44]. Bridged polysilsesquioxanes are prepared in one step from molecular starting materials and the extent of governance over bulk chemical and physical attributes has made these classes of materials exceptional candidates for applications ranging from optical device fabrication [49] to catalyst supports [53] and starting materials for ceramics [54].

“The incorporation of organic/oligomeric/polymeric materials into organic /inorganic networks by sol-gel method makes it practicable to optimize selected properties without tampering with others”. The linking of organic functional groups into an inorganic network can lead to novel structural attribute transmutations, thereby enhancing novel powerful applications for the resultant materials with distinct parts [55]. Porosity is an essential attribute of materials employed in the manufacture of catalysts, chromatographic bolsters, membranes, and adsorbent

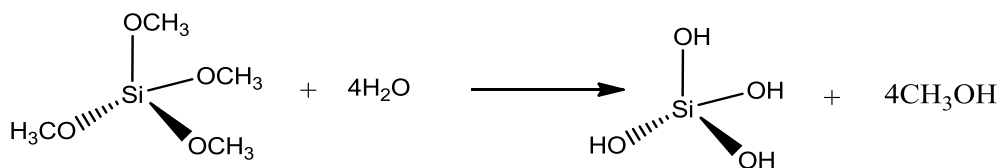
materials [47]. High surface areas and control over the pore size of materials are paramount in the synthesis of bridged polysilsesquioxanes. Porosity in bridged polysilsesquioxanes can also be made possible by using the organic functional group as a template for porosity. Templating is dependent on an organic functional group holding space until calcination, chemical oxidation, chemical rearrangements, or hydrolysis which expels the template. Template expulsion generates a pore whose size and shape almost looks like that of the organic molecule.

Ability of bridged bis-trialkoxysilanes to form mesoporous materials with stable porous structure makes the use of an inorganic linker in their polycondensations unnecessary. Thus, contents of functional groups in such materials can be significantly higher than in materials prepared by conventional co-condensation methods.

General Background of Sol-Gel Chemistry

“Sol-gel chemistry which is typically known as chemical solution deposition, is a wet chemical procedure employed to a great extent in the fields of materials science and ceramic engineering. Such methods are chiefly used for the manufacture of materials. The starting materials for most sol-gel procedures are metal alkoxides and metal chlorides, which partake in various forms of hydrolysis and polycondensation reactions” [56]. Sol-gel process is a technique employed in preparation of pure ceramic starting materials and inorganic glasses at moderately low temperatures. The reaction is typically carried out in two stages: hydrolysis of metal alkoxides to generate hydroxyl groups, accompanied by polycondensation of the hydroxyl groups, and remaining alkoxy groups to form a three-dimensional structure (Figure 4). The reaction typically initiates with alcoholic or other low molecular weight organic solutions of monomeric, metal, or metalloid alkoxide starting materials with a general formula of $M(OR)_n$,

where M is a network-forming element such as silicon, titanium, zirconium, aluminum, boron, etc., and R is an alkyl functional group and or water. The hydrolysis and condensation reactions occur simultaneously once the hydrolysis reaction has been initiated. These gives rise to byproducts with lower molar masses such as alcohol and water must be eliminated from the reaction mixture. The elimination would lead to the formation of tetrahedral SiO₂ network if M is silicon. Both hydrolysis and condensation reactions occur by nucleophilic substitution that includes three steps: adding a nucleophile, proton transfers in the transition states, and elimination of the protonated species as an alcohol or water [55].



Tetramethoxysilane

(TMOS)

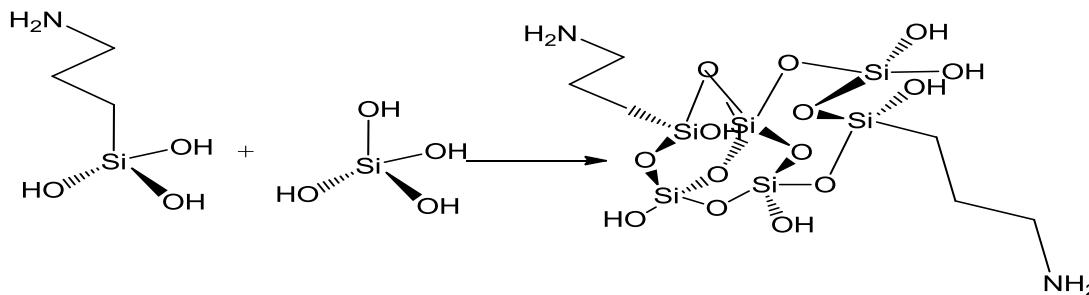


Figure 4. Typical example of a sol-gel synthesis

Research Objective

The objective of this research is to obtain porous hybrid organic-inorganic materials with high contents of amine groups and to study accessibility of these groups for different substrates of acidic nature.

CHAPTER 2

EXPERIMENTAL

Reagents

Precursor

Bis[3-(trimethoxysilyl)propyl]amine (BTMSPA, figure 5) was obtained from Sigma Aldrich (St.Louis, MO)

Surfactants

Dodecylamine (DDA, $C_{12}H_{27}N$, MW = 185.35, Figure 6) and dodecyl sulfate sodium salt (DDS, $NaC_{12}H_{25}SO_4$, MW = 288.38, Figure 7) were obtained from Acros Organics (Morris Plains, NJ)

Other Chemicals

NaOH and HCl were obtained from Acros Organics (Morris Plains, NJ)

2, 4, 6-trinitrophenol (Picric Acid, Figure 8) was obtained from Merck&Co, Inc. (Rahway, NJ).

Barium hydroxide and potassium hydrogen phthalate (KHP, Figure 9) were obtained from Fisher Scientific (NJ, USA)

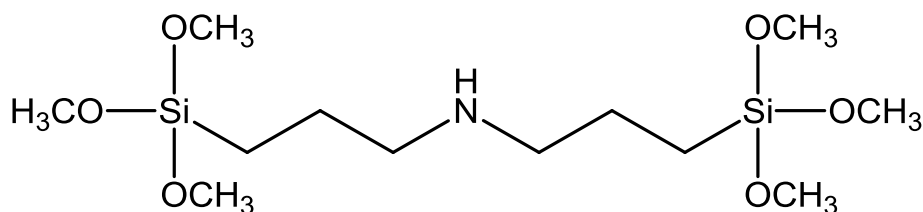


Figure 5. Structure of BTMSPA

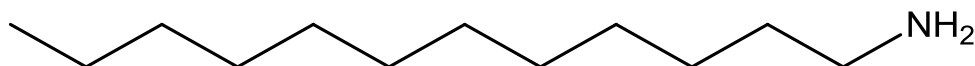


Figure 6. Structure of DDA

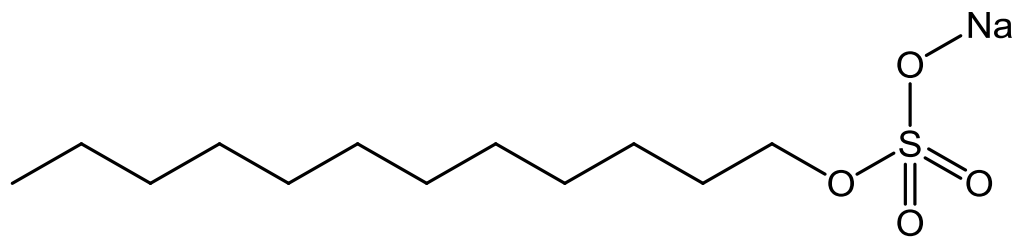


Figure 7. Structure of DDS

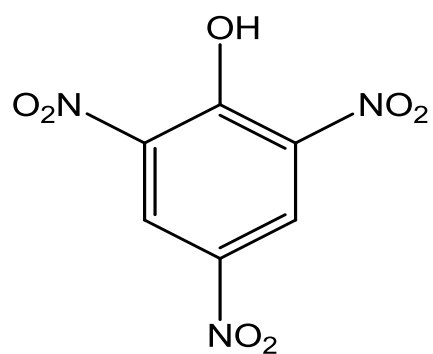


Figure 8. Structure of Picric Acid

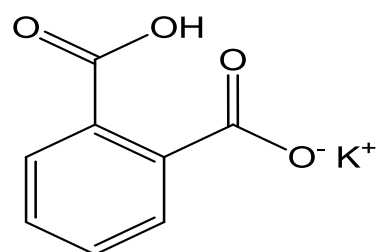


Figure 9. Structure of KHP

Preparation of Sample 1

Dodecyl sulfate sodium salt (0.214 g) was dissolved in 35 mL of distilled water with stirring on a hot plate at a temperature of 50 °C. Bis[3-(trimethoxysilyl)-propyl]amine (2.074 g) was added dropwise to the mixture from above until all portions were transferred to the surfactant while the reaction temperature was still maintained at 50 °C with continuous stirring on a hot plate for 24 h using a magnetic stirrer. The pH of the resulting mixture was found to be 11.2. Gelation of sample 1 occurred almost immediately. The product was collected and surfactant was removed by washing with distilled water until it became neutral to litmus paper. The product was allowed to dry in a fume hood and was then pulverized to a fine powder. This fine powder was washed initially with three portions of distilled water, three portions of acetone, and then washed again with another two portions of distilled water and two portions of acetone. The final product obtained was allowed to air-dry for 48 h.

Preparation of Sample 2

Dodecylamine (0.130 g) was dissolved in 33 mL of distilled water. A 0.048 M solution of HCl was also added to this mixture and stirred continuously on a hot plate and reaction temperature was set to 50 °C. The pH of the resulting mixture was found to be 3.5. Bis[3-(trimethoxysilyl)-propyl]amine (2.069 g) was added drop wise to the reaction mixture within 30 min while the reaction temperature was still maintained at 50 °C and reaction was carried out on a hot plate with continuous stirring for 24 h using a magnetic stirrer. It took 45 min for Sample 2 to form a gel unlike Sample 1 that formed a gel almost immediately. The product obtained was collected and surfactant removed by washing with distilled water until it became neutral to litmus paper. The product was pulverized to a fine powder. This fine powder was then

washed with three portions of distilled water and three portions of acetone and then further washed with another two portions of water and two portions of acetone. The final product was allowed to air-dry for 48 h.

Characterization

Elemental analysis on C, H, and N was provided by Robertson Microlit Laboratories, Inc. (Ledgewood, NJ) for both Samples.

IR spectra were recorded in pellets with KBr on a Vertex 70/80 FT-IR Spectrometer (Bruker Optics, Inc., Billerica MA).

Surface area, total pore volume, and pore size distribution were determined by BET adsorption of N₂ on a NOVA 2200e Surface Area Analyzer (Quantachrome Instruments, Boynton Beach, FL). Before the measurements, all samples were degassed for 3 hrs at 120 °C in vacuum. BET surface area was calculated from the adsorption branch of isotherms in the range of $P/P_0 = 0.2-0.5$. Pore size distribution was obtained using the BJH method.

XRD patterns were recorded on a Rigaku Miniflex X-Ray Diffraction Spectrometer using a Copper anode X-Ray tube operated at 30 kV and 15 mA. Diffraction patterns for samples 1 and 2 were collected from 2.5 degrees two theta angle to 80 degrees two theta angle with a sampling width of 0.02 degrees and a scan speed of 0.10 degrees/min.

Small-angle X-ray scattering (SAXS) experiments were performed using a Kratky camera. Copper anode emission was monochromated by total internal reflection and nickel filter. The intensity curves were recorded in the step-scanning mode of the scintillation detector. FFSAXS program [57] was used to smooth the SAXS curves, to correct them for parasitic

scattering and to carry out the desmearing procedure. The SAXS curves were recorded in the range of scattering angles from 0.03 to 4 degrees that corresponds to a wave vector, q , with values from 0.022 to 2.86 nm^{-1} . Global unified equation of Beaucage [58-60], that describes scattering from complex systems containing multiple levels of related structural features, has been used to fit measured SAXS intensity curves.

Transmission Electron Microscopy (TEM) images were obtained on a JEOL 1230 electron microscope (Tokyo, Japan) at 80 kV. Before imaging the samples were dispersed in 50 % ethanol solution on a W-385 sonicator for 2 min.

Potentiometric Titration

All titrations were carried out using an Accumet® model 25 pH/ion meter. A 0.01 M NaOH solution was standardized using a 0.01 M potassium hydrogen phthalate solution. Standardized NaOH solution was also used to determine the exact concentration of HCl used. 0.05 M HCl solution was diluted to obtain a 0.01 M solution of HCl. Sample 2 (100 mg) was degassed for 2 hrs at a temperature of 120 °C in vacuum. Degassed Sample 2 (50 mg) was shaken with 10.0 mL of distilled water to form a suspension. This mixture was covered in order to prevent the absorption of any gases from the surroundings. The suspension of material 2 obtained was titrated against a 0.01 M solution of HCl and titration was stopped when the pH of the resulting solution reached 2.15. A pH versus volume of 0.01 M HCl used data were obtained after the addition of 0.5 mL of 0.01 M HCl during each interval. The volume of 0.01 M HCl solution required for this titration was 17.0 mL. Degassed sample 2 (50 mg) was again shaken with 10.0 mL of distilled water to also form a suspension. This suspension was also covered in order to prevent the absorption of any gases from the surroundings. The suspension of material 2

obtained was titrated against 0.0265 M picric acid solution and titration was stopped when the pH of the resultant solution reached 2.16. A pH versus volume of 0.0265 M picric acid solution used data were obtained after the addition of 0.5 mL of 0.0265 M picric acid solution during each interval. The volume of picric acid required for this titration was 8.0 mL.

The same titration procedure was repeated for a blank solution where 10 mL of distilled water was titrated against 0.01 M HCl solution and the volume of HCl required for the blank solution was 0.5 mL at a resultant solution pH of 1.99. Distilled water (10 mL) was also titrated against 0.0265 M picric acid and the volume of picric acid required for the blank solution was 7.0 mL at a resultant solution pH of 2.33. Sample 1 (100 mg) was degassed for 2 hrs at a temperature of 120⁰C in vacuum. Degassed Sample (50 mg) was shaken with 10 mL of distilled water to form a suspension of the material. This mixture was covered in order to prevent the absorption of any gases from the surroundings. The suspension of material 1 obtained was titrated against a 0.01 M HCl solution and stopped when the pH of the resulting solution reached 2.19. A pH versus volume of 0.01 M HCl used data were obtained after the addition of 0.5 mL of 0.01 M HCl during each interval. The volume of 0.01 M HCl solution required for this titration was 14.0 mL. Degassed Sample 1 (50 mg) was again shaken with 10.0 mL of distilled water to also form a suspension. This suspension was also covered in order to prevent the absorption of any gases from the surroundings. The suspension of material 1 obtained was titrated against 0.0265 M picric acid solution and titration was stopped when the pH of the resultant solution reached 2.07. A pH versus volume of 0.0265 M picric acid solution used data were obtained after the addition of 0.5 mL of 0.0265 M picric acid solution during each interval. The volume of picric acid required for this titration was 6.0 mL.

CO₂ Adsorption and Desorption on Samples

The carbon dioxide adsorption/ desorption of both samples was studied by gravimetric analysis. Samples 1 and 2 (0.5 g) were transferred into a U-shaped tube and a stream of carbon dioxide was passed through these samples for 24 h to saturate the samples. In addition, a concentrated solution of barium hydroxide was prepared by dissolving 3.0 g of barium hydroxide crystals in 100 mL of distilled water. Carbon dioxide desorption was further studied by heating each sample at a temperature of 120 °C in vacuum while charging each of the samples saturated with carbon dioxide with a stream of nitrogen gas that was connected to a flask containing a concentrated solution of barium hydroxide. A precipitate of barium carbonate formed during this process which was collected and weighed.

Percentage of Water Absorbed Per Dry Samples

Samples 1 and 2 (0.204 g) were weighed and transferred into two separate 20 mL beakers. Distilled water (1 mL) was added to each of the samples to form suspensions. These suspensions were filtered; precipitate of both samples were collected on pre-weighed filter papers and allowed to air dry for 48 h with no heating. After drying, weights of both samples were recorded. These dried samples were then transferred into two separate heating tubes for degassing. Degassing of both samples was done for 6 h in vacuum at a temperature of 120 °C. After degassing, the difference in weight before and after degassing was recorded for each of the samples and the percent water absorbed per dry samples was calculated.

CHAPTER 3

RESULTS AND DISCUSSION

Synthesis of Samples

Two surfactants were selected as templates in the synthesis of Samples 1 and 2. DDS represents a group of anionic surfactants, while DDA is a cationic one. Hydrochloric acid was added to the reaction mixture during synthesis of sample 2 in order to convert DDA to the corresponding ammonium salt. In the case of DDS no base was added; however, the solution was basic due to the presence of an amine group in the molecule of the precursor. In basic media, gelation occurred almost immediately while in the presence of HCl, gelation started on after 45 min of stirring. We attribute fast gelation of the reaction mixture during the synthesis of sample 1 to the self-catalyzing effect of the precursor containing basic amine groups. Presence of HCl in the reaction mixture (sample 2) neutralized them thus reducing their catalytic effect.

Total Contents of Amino Groups

Total content of NH (secondary amine) groups in silsesquioxanes (Table 3) and the degree of hydrolysis were calculated from the data C, H, and N elemental analysis. Elemental analysis of the Samples showed that relative contents of C and H in respect to N are higher than in the amine-containing bridge (6:13:1). Thus, for Sample 1 it was 6.38:17.37:1 while for Sample 2 their ratio was 6.39:15.21:1. The excessive contents of C and H might be explained by the presence of Si-O-CH₃ groups that remained unhydrolyzed, thus increasing the contents of these elements in respect to N. In addition, a higher H content is an evidence of physisorbed and chemisorbed water.

FT-IR Spectroscopy

FT-IR spectra (Appendix F) of both samples have absorption bands attributed to inorganic and organic phases of hybrid organic-inorganic materials. The bands at 457-458 (δ_{SiO}), 779-780 (ν_{SiO}), and 1029-1127 cm^{-1} (two bands, ν_{SiOSi}) are characteristic for a silica network. Other characteristic bands of inorganic materials are referred to as silanol groups formed by the hydrolysis of Si-O-CH₃ groups in BTMSA. These bands are located at 920-923 (ν_{SiO}), 1662-1664 (δ_{HOH}), and 3400 -3600 cm^{-1} (broad band, ν_{OH}). Other bands are attributed to organic groups in the material structures. Bands of CH₂ groups are located at 1282-1283 (ω_{CH_2}), 1477-1480 (δ_{CH_2}), and 2934-2937 cm^{-1} (ν_{CH_2}). Amine group displays bands at 1418-1419 (ν_{CN}) and 1531-1533 cm^{-1} (δ_{NH}). Neither spectra contain absorption bands of SDS and DDA, and this confirms the absence of entrapped surfactants in the pores of these materials.

Porous Characteristics of Samples

Adsorption/desorption isotherms (Appendix A) of both samples show the presence of mesopores in their structures. Sample 1 displayed an isotherm of mixed II+IV type with hysteresis loop of type H2 [61]. This type of isotherm is characteristic for solids with wide pore size distributions. Sample 2 showed a BET isotherm of pure type IV with hysteresis of type H2. The pores in this sample have more narrow size distributions and exhibit the ink-bottle shape. As seen from Appendix A, it has a small fraction of larger mesopores ($R > 80 \text{ \AA}$) while contributions of such pores to the porous structure of Sample 1 is more significant. In contrast, Sample 2 has a higher fraction of micropores in its total pore volume. Surface area of Sample 2 is almost two times higher than that of Sample 1 (Table 2).

The difference in pore size distributions in the samples might be explained by different mechanisms of polycondensation in acidic and basic media. While acid-catalyzed reaction leads

to a linear polymer structure, the products of base-catalyzed reactions are highly branched dense polymers. Similar effect of reaction media on pore size distributions in inorganic silica materials was reported earlier [62].

Table 2. Porous characteristics of bridged silsesquioxanes

Sample	BET Surface Area, m ² /g	Total Pore Volume, cc/g	Micropore Volume, cc/g
1	109	0.352	0.108
2	205	0.404	0.190

X-ray Powder Diffraction Patterns of Samples

X-ray Powder Diffraction (XRD) study of the silsesquioxane structures showed similar short-range ordering. No reflections were observed in high-angle region of XRD pattern. Thus, the structures of both materials have low long-distance order. The diffraction patterns of samples 1 and 2 (Appendix D and E) are typical of amorphous materials as it is evident from the reflection at $2\theta=20.9^\circ$. The width of this reflection at half-maximum is $\sim 8^\circ$ which indicates a broad distribution of Si-O bonds and Si-O-Si angles [63]. Another broad diffraction peak corresponding to [100] reflection is observed at $2\theta=9.0^\circ$ (Sample 1) and 8.6° (Sample 2). The broadness of these peaks is due to amorphous character of the obtained hybrid materials and the presence of an organic phase. The coherent distances corresponding to this reflection was calculated from Bragg's equation:

$$n\lambda = 2d \sin \theta$$

The coherent distances equal 9.83 and 10.28 Å, respectively. It should be noted that these values correspond to the distance between Si atoms in the molecule of the precursor (BTMSA) in the

conformation with minimized energy, which is 9.842 Å. This distance was calculated using the Spartan '06 software (Appendix G).

Extremely good agreement between d-spacing values calculated from Bragg's equation and distance between Si atoms from molecular modeling is an indication of interconnection of the peak at low 2θ with arrangement of silica atoms in the structure of obtained Samples.

Small Angle X-ray Scattering of Samples

SAXS curves of both samples (Appendix H) contain two linear regions corresponding to two levels of their fractal structures. In the region $q=0.2-1.1 \text{ nm}^{-1}$ the parameter α (calculated from Porod equation $I=Cq^\alpha$) have values -3.85 and -4.00 for Samples 1 and 2, respectively. The value $\alpha=-3.85$ reflects a presence of mass fractals with Guinier radius $R_g=7.0 \text{ nm}$ (diameter of equivalent sphere $\sim 18 \text{ nm}$) and rough surface of the particles of corresponding structural level. We refer these mass fractals to mesopores in the Sample 1. In the second region $q=0.03-0.2 \text{ nm}^{-1}$ the parameter α changed to -1.7 proving agglomeration of primary structural units to anisodiametric aggregates. In the case of Sample 2, the value $\alpha=-4.00$ shows smooth surface of primary structural units. The range of the first region of SAXS curve is shorter with $q=0.4-1.1 \text{ nm}^{-1}$ due to smaller mass fractals of the first level ($R_g=4.5 \text{ nm}$ and diameter of equivalent sphere $\sim 12 \text{ nm}$). Thus, pore size of Sample 2 is smaller than that of Sample 1. On the secondary structural level, agglomeration is also detected. These data are in good agreement with porosity study using N_2 adsorption which also revealed a higher content of larger mesopores in Sample 1.

Transmission Electron Microscopy of Samples

Transmission Electron Microscopy (TEM) images of Samples 1 and 2 (Appendix B and C) reveals the spherical morphologies of the particles in both materials. The size of individual particles was in the range of 50-100 nm; however, they formed large agglomerates up to 0.5-1.5

μm . No phase separation could be observed from the images. The TEM image of Sample 1 reveals its layered structure while that of Sample 2 revealed a bulky structure.

Relative Basicity of Samples

Elemental analysis data have shown the total contents of the amine groups present in the silsesquioxanes. However, the accessibilities of these amine groups vary for different molecules depending on steric hindrance with respect to these silsesquioxanes (Samples 1 and 2). In particular, pore size and surface area significantly affect the ability of these basic sites to react with molecules of acidic nature. Thus, basicity of these materials (Samples 1 and 2) in reactions with different acidic substrates should be different. For the determination of the relative basicity we used acidic reactants of different molecular sizes such as HCl, picric acid and CO_2 .

The volume of a single molecule of picric acid is 171.06 \AA^3 (All molecular volumes were calculated using Spartan 2006 software). For comparison, the volume of a single HCl molecule is 26.02 \AA^3 . Titration by these two strong acids was carried out in order to determine the accessibility of the basic amine groups for small and large molecules in solution. Data obtained, listed in Table 4, show a notable difference in the contents of the basic sites accessible for each acid. It was found that 83.5 % of $>\text{NH}$ groups in Sample 2 were accessible for HCl while for Sample 1 this value was only 57.5 %. The accessibility for picric acid was 6.4 % in Sample 1 and 11.1 % for Sample 2, which is much lower compared to that of HCl. We can conclude that Sample 2 has a higher fraction of small micropores in its porous system.

Carbon Dioxide Adsorption

The ability of amine groups in both materials to adsorb acidic molecules in the gas phase was also studied using CO_2 adsorption and desorption. The volume of a single CO_2 molecule is

41.92 Å³. Results of the experiments showed that adsorption capacity on both samples was similar (Table 4). The total content of >NH groups accessible to CO₂ in Sample 1 was 59.3 % and 54.6 % for Sample 2.

Adsorption Capacity on Water

Hydrophilicity of obtained silsesquioxanes was estimated based on their adsorption capacity on water. Adsorption capacity on water was different for the two samples. Sample 2 adsorbed 2.7 times more water than Sample 1 (Table 3). Such a large difference can't be explained by higher surface area alone. We suggest that most of the water must have been adsorbed in the micropores, where micropore surface area can't be calculated from BET isotherms.

Table 3. Characteristics of bridged silsesquioxanes

Sample	pH of reaction mixture	Degree of hydrolysis, %	Contents of amine groups, mmol/g				Adsorption capacity on H ₂ O, %
			By elemental analysis	By HCl titration	By picric acid titration	CO ₂ adsorption	
1	11.2	93.7	3.91	2.25	0.25	2.32	3.9
2	3.5	93.5	4.49	3.75	0.5	2.45	10.5

Table 4. Results of the percent >NH groups accessible

Sample	% >NH Accessible by HCl	% >NH Accessible by Picric acid	% >NH Accessible by CO ₂
1	57.5	6.4	59.3
2	83.5	11.1	54.6

It is evident from the results of experiments that the presence of a bridge in a precursor molecule favors formation of solid polymeric structures. In contrast, polycondensation of non-bridged precursors, such as (3-aminopropyl)trimethoxysilane, yields water-soluble oligomers with low molecular weight [64]. However, the most valuable feature of bridged precursor is its stabilizing effect on a silsesquioxane mesoporous structure even at high contents of organic phase. The use of bridged amine-functionalized precursor proved to be a promising approach to obtaining highly functionalized materials with mesoporous structure.

Conclusion

Two mesoporous silsesquioxanes with high contents of amine groups were obtained in acidic and basic media. The material obtained by acid-catalyzed polycondensation had a narrow pore size distribution with higher fraction of micropores. Its high BET surface area and accessibility of amine groups makes these materials novel in development of adsorbents and heterogeneous catalysts for organic reactions.

REFERENCES

1. Environmental Defense Fund, Basics of Global Warming. The Greenhouse Effect: A Natural Balance. http://www.edf.org/climate/basics-globalwarming?gclid=CN_a1eacgKwCFQFZ7AodcTF0jw (Accessed October 23, 2011)
2. Kessel, D. G., Global warming -- facts, assessment, countermeasures. *Journal of Petroleum Science and Engineering* **2000**, 26 (1-4), 157-168.
3. Yang, H. Q.; Xu, Z. H.; Fan, M. H.; Gupta, R.; Slimane, R. B.; Bland, A. E.; Wright, I., Progress in carbon dioxide separation and capture: A review. *Journal of Environmental Sciences-China* **2008**, 20 (1), 14-27.
4. Siriwardane, R. V.; Shen, M.-S.; Fisher, E. P.; Poston, J. A., Adsorption of CO₂ on Molecular Sieves and Activated Carbon. *Energy & Fuels* **2001**, 15 (2), 279-284.
5. Przepiórski, J.; Skrodzewicz, M.; Morawski, A. W., High temperature ammonia treatment of activated carbon for enhancement of CO₂ adsorption. *Applied Surface Science* **2004**, 225 (1-4), 235-242.
6. Gray, M. L.; Soong, Y.; Champagne, K. J.; Pennline, H.; Baltrus, J. P.; Stevens, R. W.; Khatri, R.; Chuang, S. S. C.; Filburn, T., Improved immobilized carbon dioxide capture sorbents. *Fuel Processing Technology* **2005**, 86 (14-15), 1449-1455.
7. Hiyoshi, N.; Yogo, K.; Yashima, T., Adsorption characteristics of carbon dioxide on organically functionalized SBA-15. *Microporous and Mesoporous Materials* **2005**, 84 (1-3), 357-365.
8. Cinke, M.; Li, J.; Bauschlicher, C. W.; Ricca, A.; Meyyappan, M., CO₂ adsorption in single-walled carbon nanotubes. *Chemical Physics Letters* **2003**, 376 (5-6), 761-766.

9. Xu, X.; Song, C.; Miller, B. G.; Scaroni, A. W., Influence of Moisture on CO₂ Separation from Gas Mixture by a Nanoporous Adsorbent Based on Polyethylenimine-Modified Molecular Sieve MCM-41. *Industrial & Engineering Chemistry Research* **2005**, *44* (21), 8113-8119.
10. Gao, W.; Butler, D.; Tomasko, D. L., High-Pressure Adsorption of CO₂ on NaY Zeolite and Model Prediction of Adsorption Isotherms. *Langmuir* **2004**, *20* (19), 8083-8089.
11. Siriwardane, R. V.; Shen, M.-S.; Fisher, E. P.; Losch, J., Adsorption of CO₂ on Zeolites at Moderate Temperatures. *Energy & Fuels* **2005**, *19* (3), 1153-1159.
12. Thambimuthu, K.; Soltanich, M.; Abanades, J.M. Intergovernmental Panel on Climate Change (IPCC) Special Report on Carbon dioxide Capture and Storage: Capture of CO₂, p 15.
13. Master of Science Thesis of Jak Tanthana, *Study of Amine impregnated on silica support for CO₂ capture*, August **2008**, p 2,3,15&17 (The University of Akron, Ohio)
14. Choi, S.; Drese, J. H.; Jones, C. W., Adsorbent Materials for Carbon Dioxide Capture from Large Anthropogenic Point Sources. *Chemsuschem* **2009**, *2* (9), 796-854.
15. Caplow, M., Kinetics of carbamate formation and breakdown. *Journal of the American Chemical Society* **1968**, *90* (24), 6795-6803.
16. Sartori, G.; Savage, D. W., STERICALLY HINDERED AMINES FOR CO₂ REMOVAL FROM GASES. *Industrial & Engineering Chemistry Fundamentals* **1983**, *22* (2), 239-249.
17. Donaldson, T.; Nguyen, Y. N. Carbon Dioxide Reaction Kinetics and Transport in Aqueous Amine Membranes. *Ind.Eng. Chem. Fundam.* **1980**, *19* (3), 260-266.

18. Vaidya, P. D.; Kenig, E. Y., CO₂-alkanolamine reaction kinetics: A review of recent studies. *Chemical Engineering & Technology* **2007**, *30* (11), 1467-1474.
19. Institute of Materials Chemistry, Vienna University of Technology.
http://www.imc.tuwien.ac.at/staff/acus_usiohm_e.php (Accessed April 2, 2011)
20. Yang, Q.; Liu, J.; Zhang, L.; Li, C. Functionalized Periodic Mesoporous Organosilicas for Catalysis. *J. Mater. Chem.* **2009**, *19* (14), 1945-1955.
21. Clark, J. H.; Macquarrie, D. J.; Tavener, S. J. The Application of Modified Mesoporous Silicas in Liquid Phase Catalysis. *Dalton Trans.* **2006**, *36*, 4297-4309.
22. Walcarius, A.; Mercier, L. Mesoporous Organosilica Adsorbents: Nanoengineered Materials for Removal of Organic and Inorganic Pollutants. *J. Mater. Chem.*, **2010**, *20* (22), 4478-4511.
23. N. Husing, Porous hybrid materials, in: G. Kickelbick (Ed.), *Hybrid Materials: Synthesis, Characterization, and Applications*, Wiley-VCH, Weinheim, **2007**, pp 175-224.
24. Hoffmann, F.; Cornelius, M.; Morell, J.; Froba, M. Silica-Based Mesoporous Organic-Inorganic Hybrid Materials. *Angew. Chem. Int. Ed.*, **2006**, *45* (20), 3216-3251.
25. Husing, N. Porous Inorganic-Organic Hybrid Materials. In *Functional Hybrid Materials*; Gomez-Romero, P., Eds.; Wiley-VCH; Winheim, **2004**; pp 89-103.
26. Kaneko, Y.; Iyi, N.; Kurashima, K.; Matsumoto, T. Hexagonal-Structured Polysiloxane Material Prepared by Sol-Gel Reaction of Aminoalkyltrialkoxysilane without Using Surfactants. *Chem. Mater.*, **2004**, *16* (18), 3417-3423.

27. Kaneko, Y.; Iyi, N.; Matsumoto, T.; Fujii, K.; Kurashima, K.; Fujita, T. synthesis of ion-exchangeable layered polysiloxane by sol-gel reaction of amino alkyltrialkoxysilane: a New preparation method for layered polysiloxane materials. *J.Mater.Chem.*, **2003**, *13* (9), 2058-2060.
28. Da trindade, C. M.; Stoll, G. C.; Pereira, A. S.; Costa, T. M. H.; Benvenuti, E. V. An Innovative Series of Layered Nanostructured Aminoalkylsilica Hybrid Material. *J. Braz. Chem. Soc.*, **2009**, *20* (4), 737-743.
29. Han, L.; Chen, Q.; Wang, Y.; Gao, C.; Che, S. Synthesis of Amino Group Functionalized Monodispersed Mesoporous Silica Nanospheres Using Anionic Surfactant. *Microporous Mesoporous Materials*, **2011**, *139* (1-3), 94-103.
30. Huang, H. Y.; Yang, R. T.; Chinn, D.; Munson, C. L., Amine-Grafted MCM-48 and Silica Xerogel as Superior Sorbents for Acidic Gas Removal from Natural Gas. *Industrial & Engineering Chemistry Research* **2002**, *42* (12), 2427-2433.
31. Khatri, R. A.; Chuang, S. S. C.; Soong, Y.; Gray, M., Carbon Dioxide Capture by Diamine-Grafted SBA-15: A Combined Fourier Transform Infrared and Mass Spectrometry Study. *Industrial & Engineering Chemistry Research* **2005**, *44* (10), 3702-3708.
32. Xu, X. C.; Song, C. S.; Andresen, J. M.; Miller, B. G.; Scaroni, A. W., Novel polyethylenimine-modified mesoporous molecular sieve of MCM-41 type as high-capacity adsorbent for CO₂ capture. *Energy & Fuels* **2002**, *16* (6), 1463-1469.
33. Knowles, G. P.; Graham, J. V.; Delaney, S. W.; Chaffee, A. L., Aminopropyl-functionalized mesoporous silicas as CO₂ adsorbents. *Fuel Processing Technology* **2005**, *86* (14-15), 1435-1448.

34. Knowles, G. P.; Delaney, S. W.; Chaffee, A. L., Diethylenetriamine[propyl(silyl)]-Functionalized (DT) Mesoporous Silicas as CO₂ Adsorbents. *Industrial & Engineering Chemistry Research* **2006**, *45* (8), 2626-2633.
35. Harlick, P. J. E.; Sayari, A., Applications of Pore-Expanded Mesoporous Silica. 5. Triamine Grafted Material with Exceptional CO₂ Dynamic and Equilibrium Adsorption Performance. *Industrial & Engineering Chemistry Research* **2007**, *46* (2), 446-458.
36. Zhao, G.; Aziz, B.; Hedin, N., Carbon dioxide adsorption on mesoporous silica surfaces containing amine-like motifs. *Applied Energy* **2010**, *87* (9), 2907-2913.
37. Pirngruber, G. D.; Cassiano-Gaspar, S.; Louret, S.; Chaumonnot, A.; Delfort, B., Amines immobilized on a solid support for postcombustion CO₂ capture-A preliminary analysis of the performance in a VSA or TSA process based on the adsorption isotherms and kinetic data. *Energy Procedia* **2009**, *1* (1), 1335-1342.
38. Bhagiyalakshmi, M.; Anuradha, R.; Park, S. D.; Jang, H. T., Octa(aminophenyl)silsesquioxane fabrication on chlorofunctionalized mesoporous SBA-15 for CO₂ adsorption. *Microporous and Mesoporous Materials* **2010**, *131* (1-3), 265-273.
39. Gray, M. L.; Champagne, K. J.; Fauth, D.; Baltrus, J. P.; Pennline, H., Performance of immobilized tertiary amine solid sorbents for the capture of carbon dioxide. *International Journal of Greenhouse Gas Control* **2008**, *2* (1), 3-8.
40. Zelenak, V.; Halamova, D.; Gaberova, L.; Bloch, E.; Llewellyn, P., Amine-modified SBA-12 mesoporous silica for carbon dioxide capture: Effect of amine basicity on sorption properties. *Microporous and Mesoporous Materials* **2008**, *116* (1-3), 358-364.

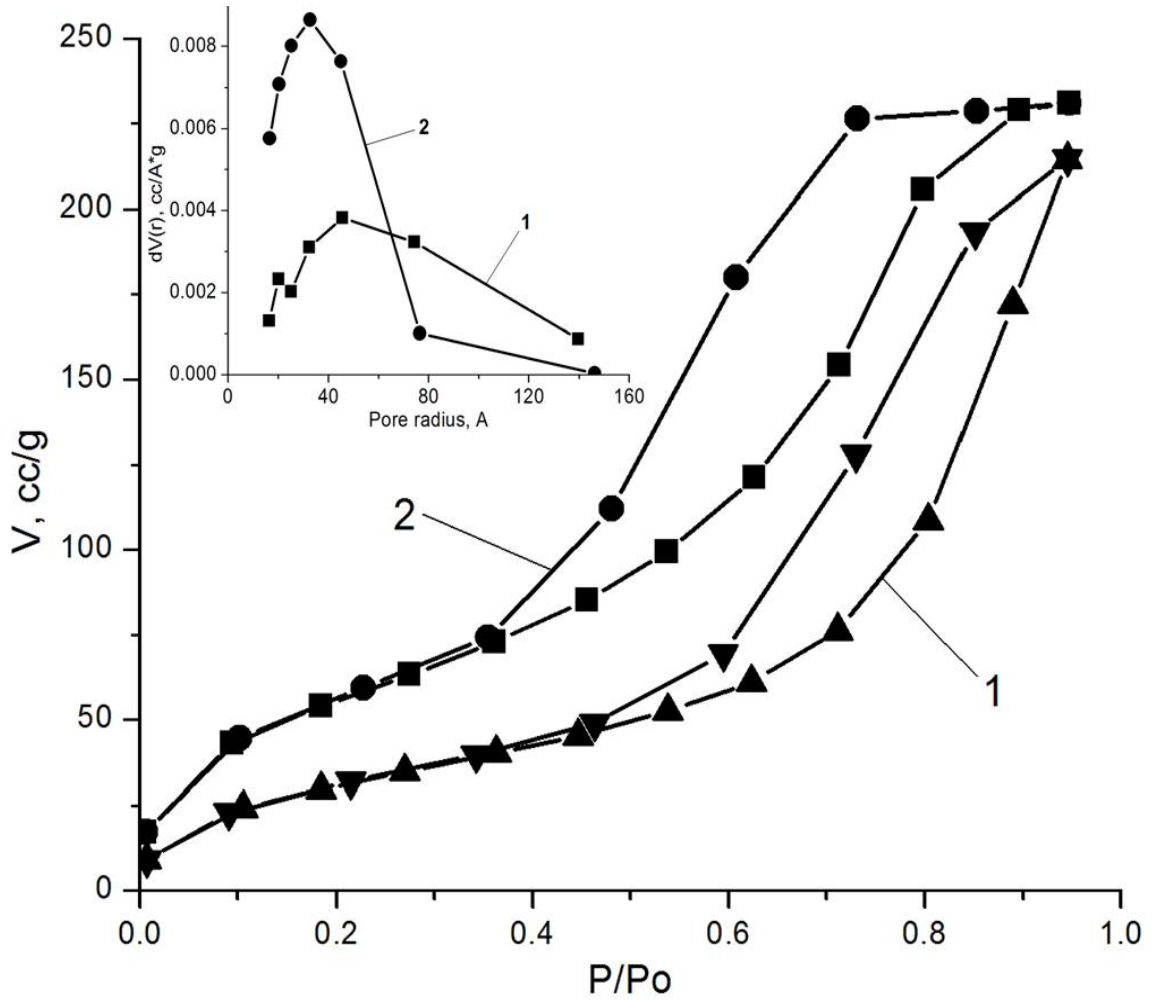
41. Kim, S.; Ida, J.; Guliants, V. V.; Lin, Y. S., Tailoring Pore Properties of MCM-48 Silica for Selective Adsorption of CO₂. *The Journal of Physical Chemistry B* **2005**, *109* (13), 6287-6293.
42. Hiyoshi, N.; Yogo, K.; Yashima, T., Adsorption of Carbon Dioxide on Amine Modified SBA-15 in the Presence of Water Vapor. *Chemistry Letters* **2004**, *33* (5), 510-511.
43. Hiyoshi, N.; Yogo, K.; Yashima, T., Adsorption characteristics of carbon dioxide on organically functionalized SBA-15. *Microporous and Mesoporous Materials* **2005**, *84* (1-3), 357-365
44. Shea, K. J.; Loy, D. A., Bridged Polysilsesquioxanes. Molecular-Engineered Hybrid Organic-Inorganic Materials. *Chemistry of Materials* **2001**, *13* (10), 3306-3319.
45. Loy, D. A.; Shea, K. J. Bridged Polysilsesquioxanes. Highly Porous Hybrid Organic-Inorganic Materials. *Chem. Rev.* **1995**, *95* (5), 1431-1442.
46. Shea, K. J.; Loy, D. A.; Webster, O., Arylsilsesquioxane gels and related materials. New hybrids of organic and inorganic networks. *Journal of the American Chemical Society* **1992**, *114* (17), 6700-6710.
47. Barton, T. J.; Bull, L. M.; Klemperer, W. G.; Loy, D. A.; McEnaney, B.; Misono, M.; Monson, P. A.; Pez, G.; Scherer, G. W.; Vartuli, J. C.; Yaghi, O. M., Tailored Porous Materials. *Chemistry of Materials* **1999**, *11* (10), 2633-2656.
48. Judeinstein, P.; Sanchez, C., Hybrid organic-inorganic materials: a land of multidisciplinary. *Journal of Materials Chemistry* **1996**, *6* (4), 511-525.
49. Cerveau, G.; Corriu, R. J. P. Some recent developments of polysilsesquioxanes chemistry for material science. *Coordination Chemistry Reviews* **1998**, *178-180* (2) , 1051-1071.

50. Hunks, W. J.; Ozin, G. A. Challenges and Advances in the Chemistry of Periodic Mesoporous Organosilicas (PMOs). *J. Mater. Chem.*, **2005**, *15* (35-36), 3716-3724.
51. Wahab, M. A.; Kim, I.; Ha, C-S. Bridged Amine-Functionalized Mesoporous Organosilica Materials from 1,2-Bis(trimethoxysilyl)ethane and Bis[(3-trimethoxysilyl)propyl]amine. *Journal of Solid State Chemistry*, **2004**, *177* (10), 3439-3447.
52. Barczak, M.; Borowski, P.; Dabrowski, A. Structure-Adsorption Properties of Ethylene-Bridged Polysilsesquioxanes and Polysiloxanes Functionalized with Different Groups. *Coll. Surf. A.*, **2009**, *347* (1-3), 114-120.
53. Schubert, U., Catalysts made of Organic-Inorganic Hybrid Materials. *New J. Chem.* **1994**, *18* (10), 1049-1058.
54. Corriu, R. J. P., Ceramics and Nanostructures from Molecular Precursors. *Angewandte Chemie International Edition* **2000**, *39* (8), 1376-1398
55. Wen, J.; Wilkes, G. L., Organic/Inorganic Hybrid Network Materials by the Sol-Gel Approach. *Chemistry of Materials* **1996**, *8* (8), 1667-1681.
56. Kokate.; Jalapure.; Hurakadle. Textbook of Pharmaceutical Biotechnology.; A division of Reed Elsevier India Private Limited, New Delhi, **2011**; p 283.
57. Vonk, C.G. FFSAXS's Program for Processing of Small-Angle X-ray Scattering Data. Geleen: DSM, **1974**.
58. Beaucage, G. Approximations Leading to a Unified Exponential/Power-Law Approach to Small-Angle Scattering. *J. Appl. Cryst.* **1995**, *28* (6), 717-728.
59. Beaucage, G. Small-Angle Scattering from Polymeric Mass Fractals of Arbitrary Mass-Fractal Dimension. *J. Appl. Cryst.* **1996**, *29* (2), 134-146.

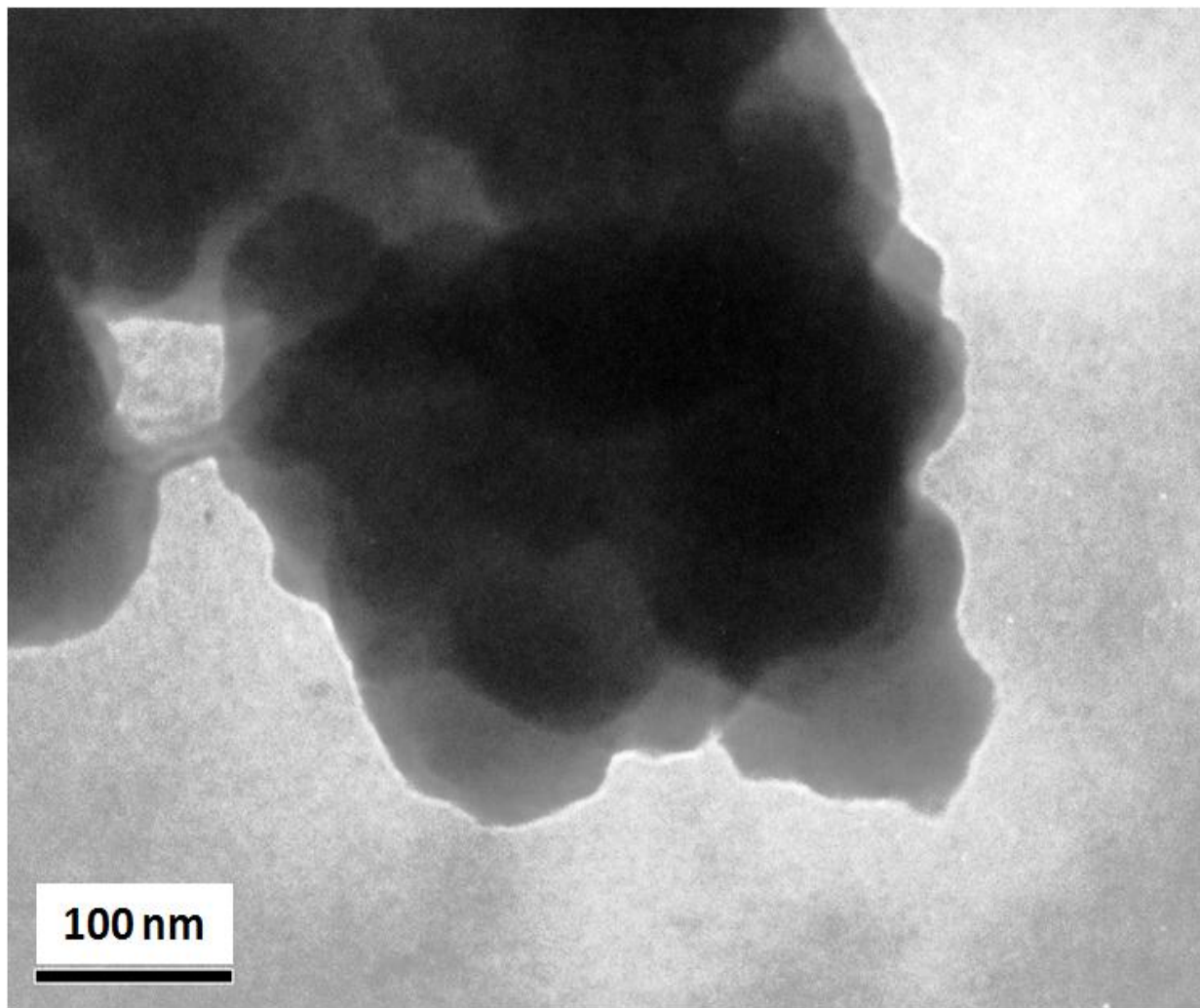
60. Hyeon-Lee, J.; Beaucage, G.; Prausnitz, S.E.; Vemury, S. Fractal Analysis of Flame-Synthesized Nanostructured Silica and Titania Powders Using Small-Angle X-ray Scattering. *Langmuir*. **1998**, *14* (20), 5751-5756.
61. Sing, K.S.W.; Everett, D.H.; Haul, R.A.W.; Moscou, L.; Pierotti, R.A.; Rouquerol, J.; Siemieniewska, T. Reporting Physisorption Data for Gas/Solid Systems with Special Reference to the Determination of Surface Area and Porosity. *Pure & Appl. Chem.* **1985**, *57* (4), 603-619.
62. Tilgner, I. C.; Fischerb, P.; Bohnena, F. M.; Rehageb, H.; Maier, W. F., Effect of Acidic, Basic and Fluoride-Catalyzed Sol-Gel Transitions on The Preparation of Sub-Nanostructured Silica. *Microporous Materials* **1995**, *5* (1-2), 77-90.
63. Larsen, G.; Lotero, E.; Marquez, M. Use of Polypropyleneimine Tetrahexacontaamine (DAB-Am-64) Dendrimer as a Single-Molecule Template to Produce Mesoporous Silicas. *Chemistry of Materials* **2000**, *12* (6), 1513-1515.
64. Khatib, I. S.; Parish, R. V., Insoluble Ligands and their Applications: A comparison of Silica-Immobilized Ligands and Functionalized Polysiloxanes. *Journal of Organometallic Chemistry* **1989**, *369* (1), 9-16.

APPENDICES

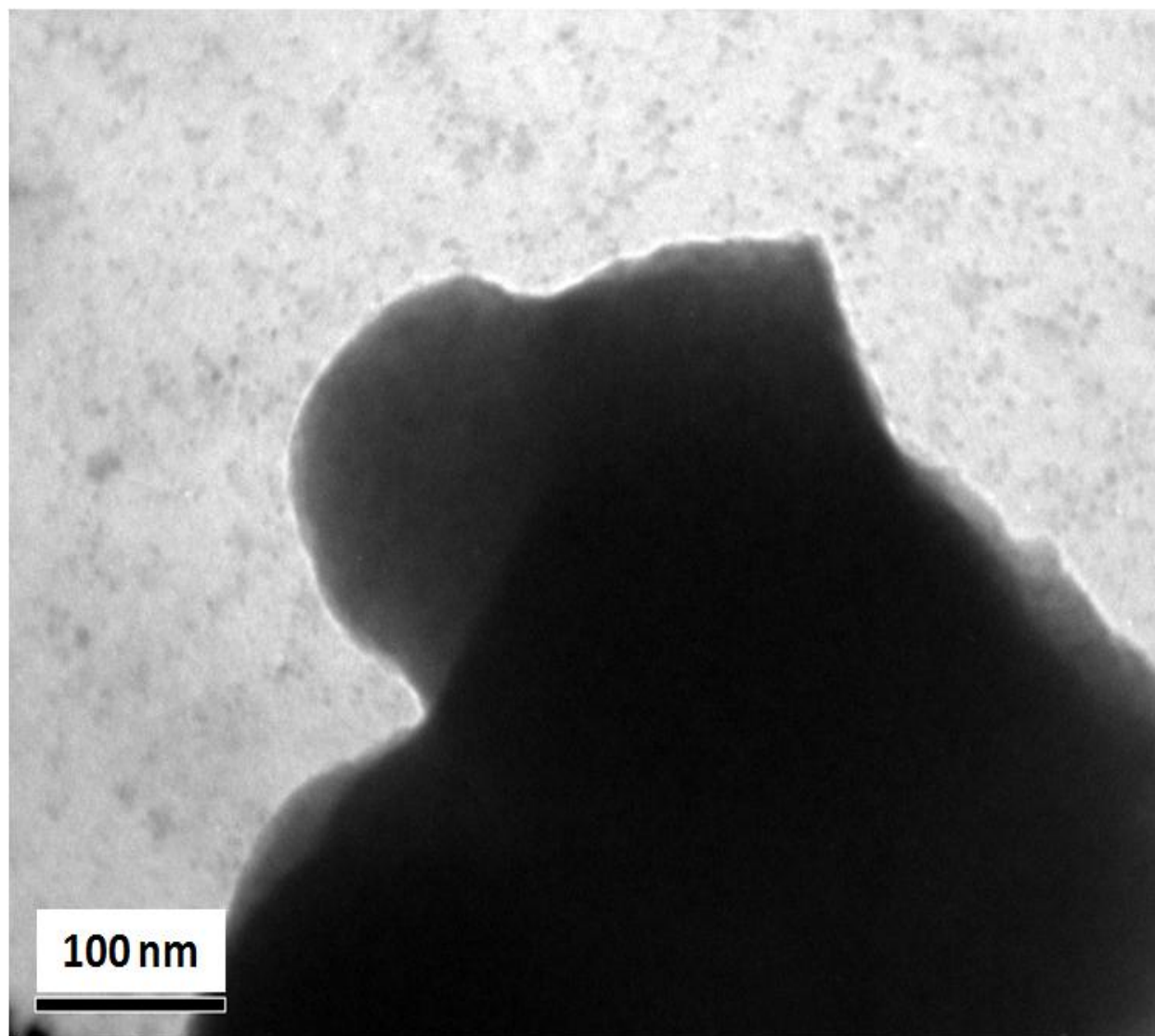
APPENDIX A. BET Adsorption Isotherms for Samples 1&2



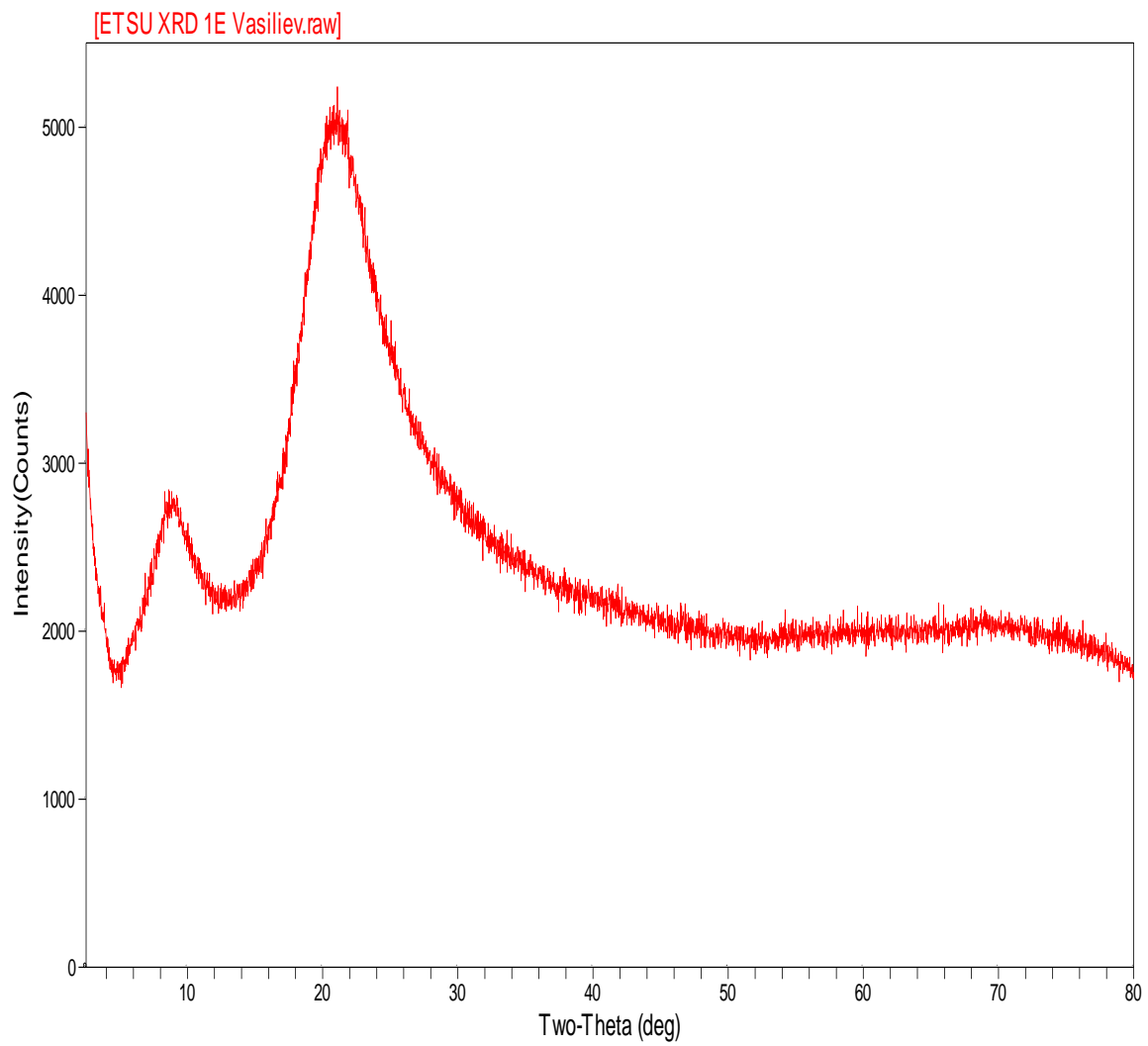
APPENDIX B. TEM Image of Sample 1



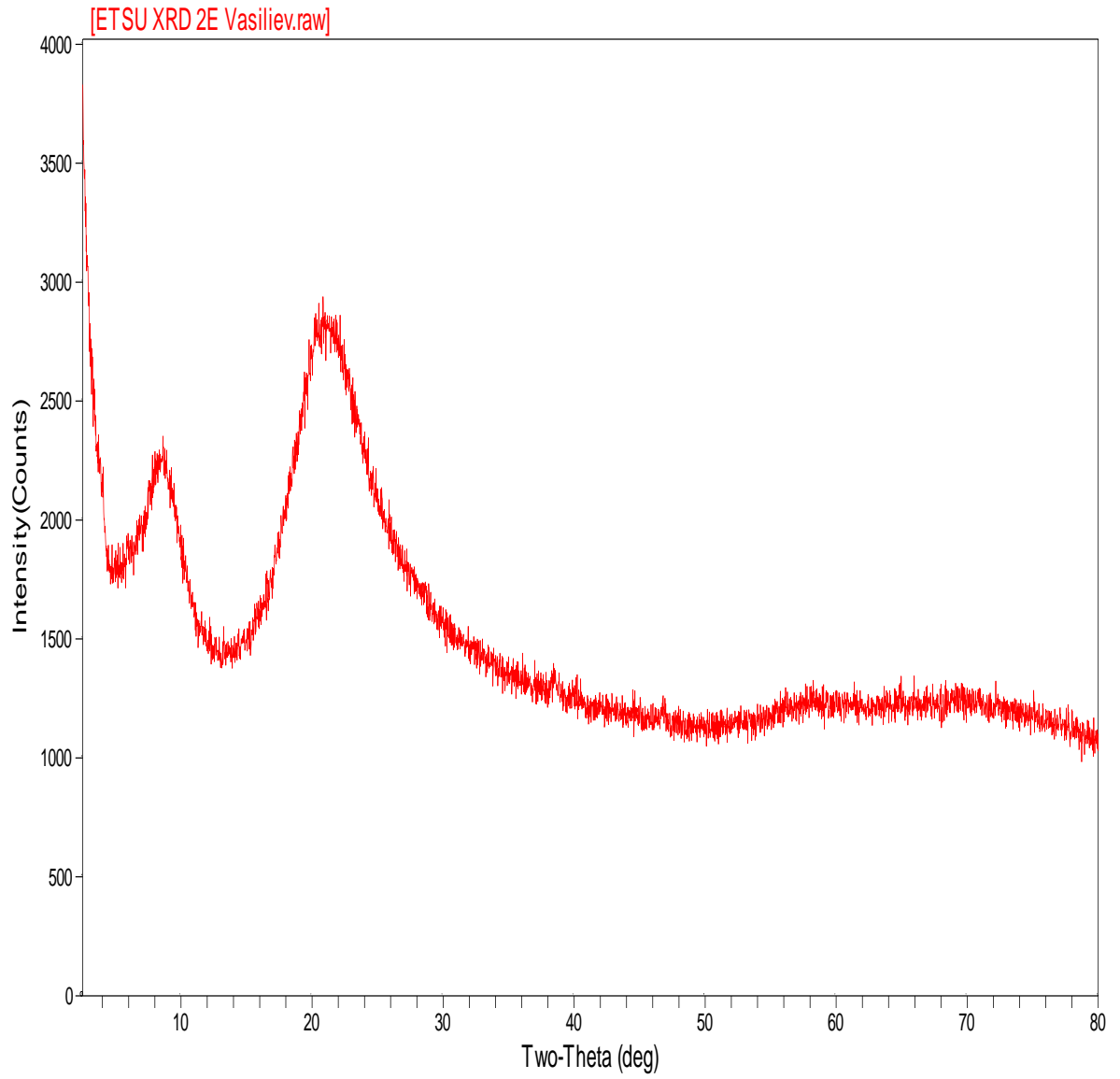
APPENDIX C. TEM Image of Sample 2



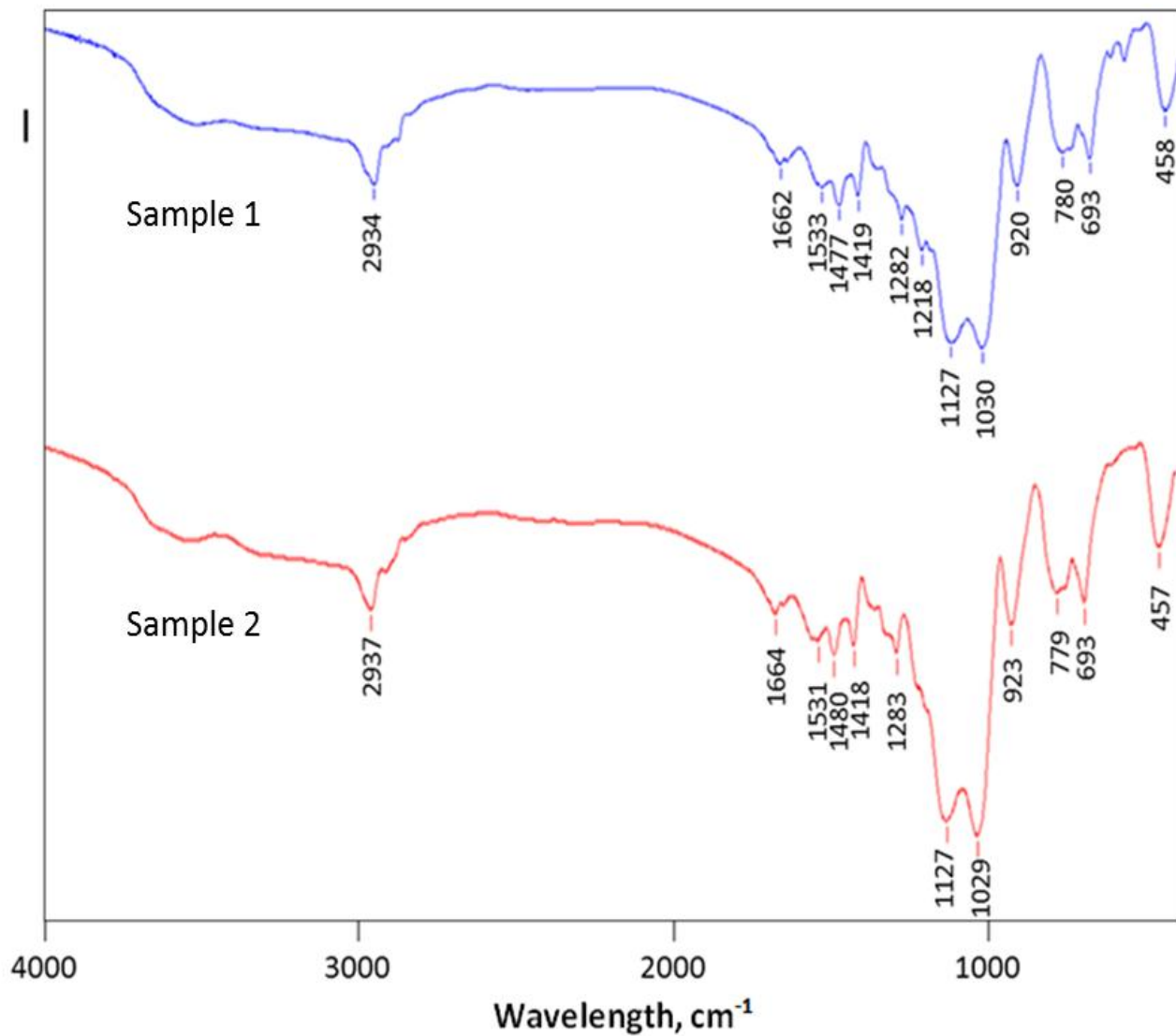
APPENDIX D. X-Ray Powder Diffractogram for Sample 1



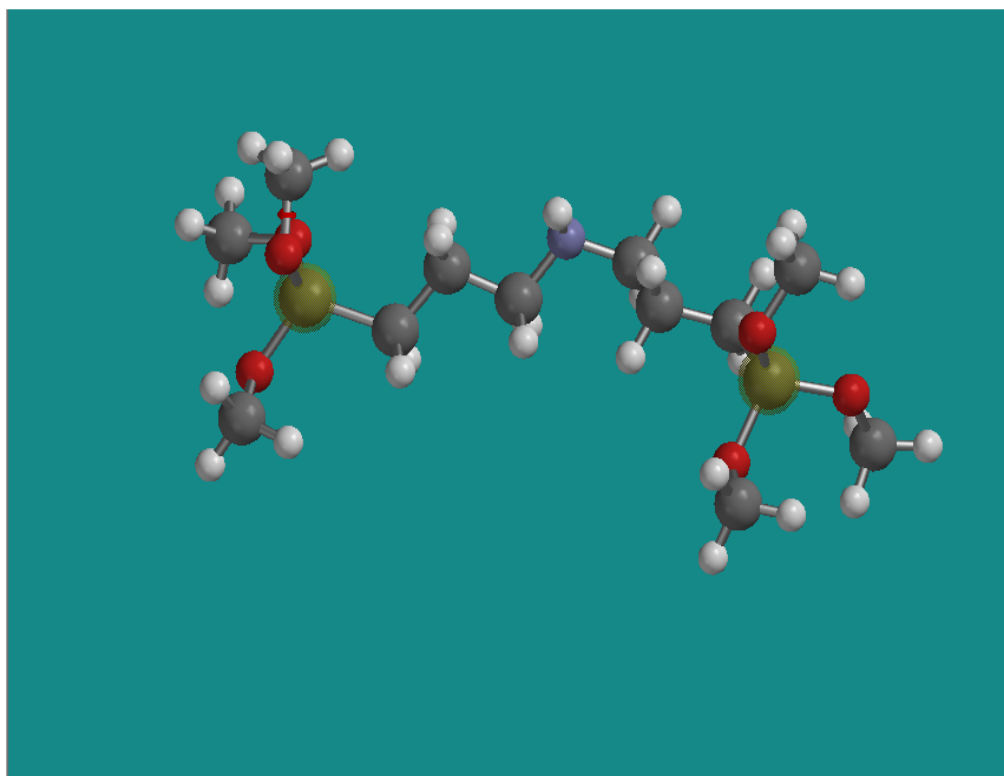
APPENDIX E. X-Ray Powder Diffractogram for Sample 2



APPENDIX F. FR-IR Spectra for Samples **1&2**

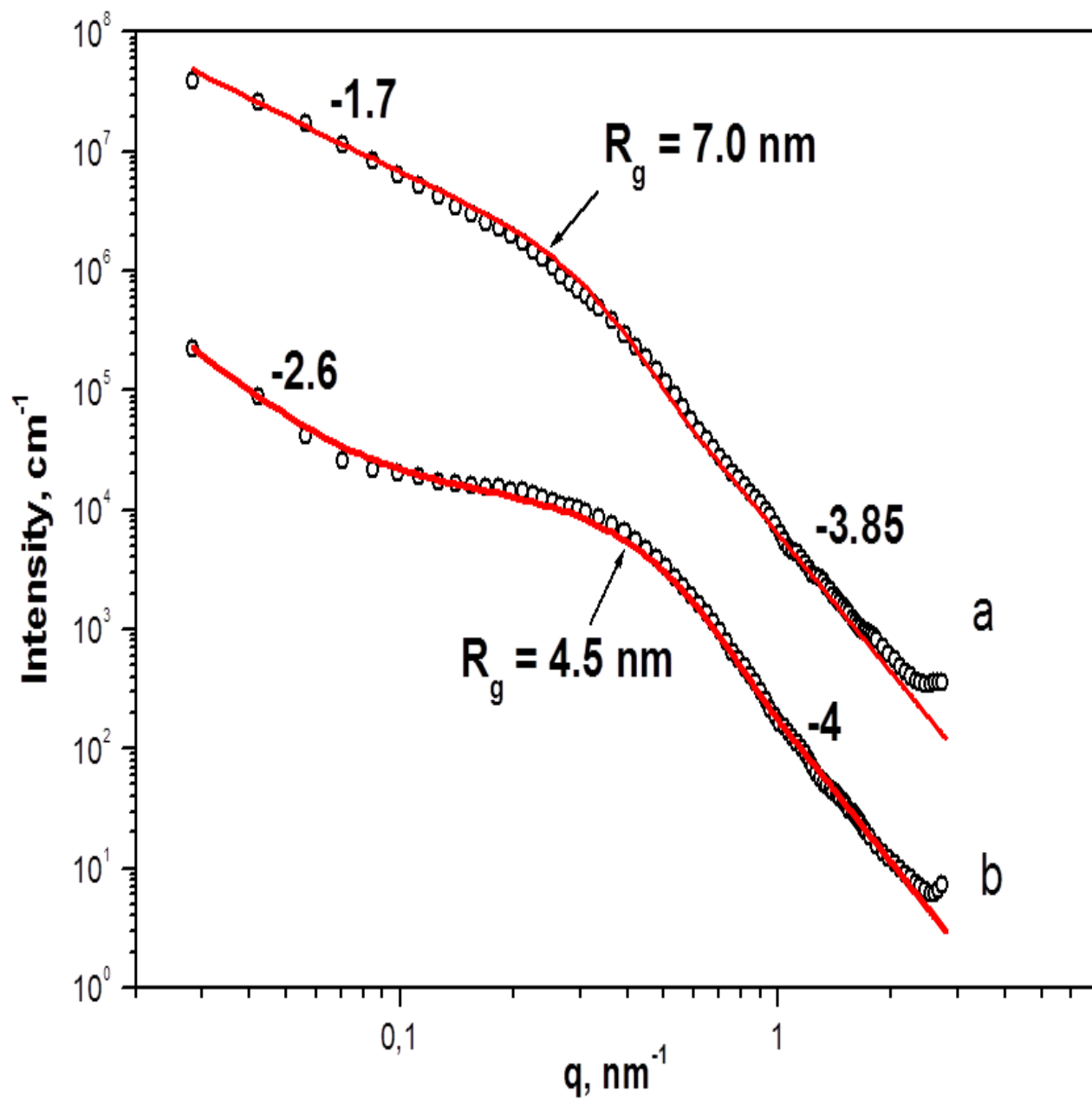


APPENDIX G. Confirmation of the Molecule of BTMSA in the Conformation with Minimized Energy



APPENDIX H. SAXS Curves of Samples 1& 2

a-1 and b-2



VITA

KOLADE OMONIYI OJO

- Personal Data: Date of Birth: April 06, 1981
- Place of Birth: Ikeja, Lagos, Nigeria
- Marital Status: Single
- Education: High School, Air Force Secondary School Kaduna, Nigeria.
 1993-1998
- B.Sc. Chemistry, Ahmadu Bello
 University (ABU), Zaria, Nigeria, 2003.
- M.S. Chemistry, East Tennessee State University (ETSU), Johnson
 City, Tennessee, 2011
- Professional Experience: Teacher, Braintrust International College Kaduna, Nigeria.
 2003.
- Teacher, Savior Model College Maiduguri, Borno State, Nigeria,
 2003-2004
- Temporary Graduate Assistant, Ahmadu Bello University Zaria,
 Nigeria, 2005
- Relationship Officer, United Bank for Africa Plc, Kaduna State,
 Nigeria, 2006-2008
- Relationship Officer, First City Monument Bank Plc, Kaduna
 State, Nigeria, 2008-2009
- Graduate Assistant at ETSU
 Johnson City, Tennessee, 2010-2011
- Awards: Outstanding Chemistry Student, Dept. of Chemistry Ahmadu Bello
 University Zaria, Nigeria.

Recipient of the Federal Government of Nigeria Scholarship.

2011 Recipient of the Margaret Sells Endowed Scholarship at ETSU as an outstanding Masters in Chemistry Student, based on scholastic Achievement.

Research Experience: Isolation of Some Active Ingredients from the Aerial Parts of ‘Cissus Rufescence’, a Medicinal Plant which is Widespread in Tropical Africa (Ahmadu Bello University Zaria, Nigeria)

Mesoporous Functionalized Materials for Post-Combustion CO₂ Capture (East Tennessee State University Johnson City, TN USA)

Publication: Ojo, K.O.; Golovko, L.V.; Gomza, Y.P.; Vasilieve, A.N. Mesoporous Materials with High Contents of Surface Amine Groups. (In View)